JIMMA UNIVERSITY

JIMMA INSTITUTE OF TECHNOLOGY

Faculty of Electrical and Computer Engineering

Communication Stream

Performance Analysis of Downlink MIMO-NOMA-Based Visible Light Communication System

A Thesis Submitted to Jimma Institute of Technology School of Graduate Studies in Partial Fulfillment of the Requirements for Masters Degree in Communication Engineering

BY

Gemechu Tesfaye Tola

August, 2021

Jimma, Ethiopia

JIMMA UNIVERSITY

JIMMA INSTITUTE OF TECHNOLOGY

Faculty of Electrical and Computer Engineering

Communication Stream

Performance Analysis of Downlink MIMO-NOMA-Based Visible Light Communication System

A Thesis Submitted to Jimma Institute of Technology School of Graduate Studies in Partial Fulfillment of the Requirements for Masters Degree in Communication Engineering

BY

Gemechu Tesfaye Tola

Main Advisor: Dr. Kinde Anlay

Co-advisor: Mr. Sherwin Catolos (Msc)

August, 2021

Jimma, Ethiopia

APPROVAL

This is to certify that the thesis prepared by **Mr. Gemechu Tesfaye Tola** entitled **"Performance Analysis of Downlink MIMO-NOMA-Based Visible Light Communication System"** and submitted as partial fulfillment for the award of the Degree of Master of Science in Electrical and Computer Engineering (Communication Engineering) complies with the regulations of the university and meets the accepted standards with respect to standards for originality, content, and quality.

Signed by Examining Board:

External Examiner: Signature, Date

Dr. Yihenew Wondie   11/08/2021

Internal Examiner: Signature, Date

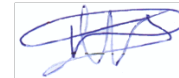Dr. Mulugeta Atlabachew   15/08/2021

Chairperson: Signature, Date

DECLARATION

I hereby declare that this thesis entitled "**Performance Analysis of Downlink MIMO-NOMA-Based Visible Light Communication System**" was prepared by me, with the guidance of my advisors. The work contained herein is my own except where explicitly stated otherwise in the text. In whole or in part, this work has not been submitted for any other degree or professional qualification.

Author: Signature, Date

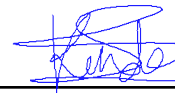Gemechu Tesfaye Tola   02/08/2021

Name of student main advisor: Signature, Date

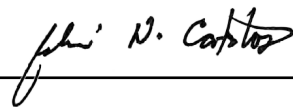Dr. Kinde Anlay   06/08/2021

Name of student co-advisor: Signature, Date

ENGR. SHERWIN N. CATOLOS   03/08/2021

DEDICATION

To those COVID-19 fighter Nurses all over the world...

ABSTRACT

Recently, visible light communication networks have emerged as a possible option for data access, primarily for indoor environments. The very high data rates, free from radio frequency interference, and low implementation cost behavior make them attractive for the next generation of indoor networking. But visible light communication technology supports only short-range data transmission, and hence the achievable data rate decreases rapidly with increasing distance between the transmitter and receiver. Additionally, developing a high data rate link in VLC system is difficult due to the narrow modulation bandwidth of LEDs. So that, it is essential to apply MIMO and Non-orthogonal Multiple Access to overcome such problems.

In this thesis, a low complexity and efficient power allocation strategy was proposed for indoor downlink MIMO-based visible light communication systems. Non-Orthogonal Multiple Access was applied on MIMO-VLC system to improve performance of edge users. Generally, the performance of the total sum rate of 4×4 MIMO VLC of k number of users were analyzed. Specifically, the sum rate, the sum rate gain, and the achievable rate of uniformly distributed users were analyzed for different power allocation techniques. MATLAB simulation results depicted that the effectiveness of the proposed power allocation strategy than gain ratio power allocation schemes and normalized gain difference power allocation schemes for the large number of users. The proposed NOMA, NGDPA, and GRPA achieved a sum rate of 261.89 Mbit/s, 235.28 Mbit/s and 152.27 Mbit/s respectively at the edge of the system for six users. More specifically, the proposed NOMA attained an achievable sum rate of 18.36% and 65.98% as compared with the NGDPA approaches, and GRPA approaches in the 4×4 MIMO based visible light communication networks with eight uniformly distributed users. The future works can focus on finding the optimal user grouping and allocating power to each group. Additionally, allocating the power according to quality of service is an open research problem in MIMO-NOMA-based VLC networks.

Key Words: *Non-Orthogonal Multiple Accesses, Multiple Input Multiple Output,Visible Light Communication, Power allocation strategy, Achievable sum rate*

ACKNOWLEDGMENT

TABLE OF CONTENTS

LIST OF FIGURES

LIST OF TABLES

LIST OF ACRONYMS

NOMENCLATURE

A_{PD} . . . . Active area of PD

Bw . . . . Transmission bandwidth

d . . . . LOS distance between the ith LED and the jth PD of the kth user

G . . . . Open-loop Voltage Gain

g_m . . . . FET Transconductor

$h_{ji,k}$ . . . . LOS channel gain between the ith LED and the jth PD of the kth user

H_k . . . . Channel gain matrix

I_2 . . . . Noise bandwidth factor

I_{bg} . . . . Photo current due to background radiation

I_{DC} . . . . DC bias current provided to each LED

K . . . . Boltzmann constant

m . . . . Lambertian emission order

n . . . . Internal refractive index of the concentrator

$n_{j,k}$ . . . . Additive Gaussian Noise

N_k . . . . Additive white noise vector

P_{opt} . . . . Optical output power

P_{rx} . . . . Received optical power for k^{th} user

q . . . . Electronic charge

$s_{i,k}$ . . . . Modulated message signal intended for the kth user from the ith LED

CHAPTER 1

1   Introduction

1.1   Introduction

As demand for wireless data services exponentially increased in recent years, it has posed several challenging issues to the existing wireless technologies. In the last few decades, we have seen an abrupt increase in the number of mobile users requiring access to high data rate wireless services everywhere over the world. This ultimate growth motivates mobile operators and standardization bodies to continuously find and develop new transmission technologies, network infrastructure solutions, protocols, and standards to enhance and achieve mobile subscriber demand. Future wireless technologies including, cognitive networks, wireless sensor networks, vehicular communications networks, and delay tolerant networks will require reliable and high data rate connections. Obviously, in such networks, spectral efficiency is an important performance metric related to the quality of service (QoS) and it has attracted significant attention from the research community and becomes one of the major concerns.

Different research groups forecasts by 2023, the total number of mobile terminals which are internet-connected will be around 29.3 billion [2]. A number of cloud based and different multi-media services operated through those terminals, for example, watching high definition online streams, enormous data throughputs that consume cloud storage, and different voice-over internet services. Forecasts show that around 77 Zeta bytes of data size will be generated by 2023 [1]-[3]. Mobile devices begin to support high data consumed applications, including augmented reality, virtual reality, and real time video communication accessing mobile terminals increasing nowadays [4, 5]. Such rapidly growing mobile user's data traffic raises a significant question on the current radio frequency communication networks, i.e., the 4G, Wireless Fidelity, and even 5G mobile networks, and many scholars agree that such technologies cannot satisfy those user's data rate demands [6, 7]. Organizations and industries have begun a new mobile technology generation called 6G mobile wireless networks to solve this situation.

Activities linked with high data rate wireless traffic are stationary and typically occurred in fixed wireless access scenarios. Reported data demonstrate that a more significant part of IP traffic service happens an indoor environments (80% indoors and only 20% of the traffic is served outdoors) [2]. The 59% of the cellular network will be offloaded to Wi-Fi by 2022. It is expected that more of the organizations would switch cellular providers by 2022 for better indoor coverage [1, 2]. This status leads to giving attention for visible light communication systems.

Visible Light Communication technology is part of the optical wireless communications. A visible light communication system transfers information through radiation over the visible light spectrum range. A visible light communication channel is not the same as radio frequency or any other communication technology in view of its properties. Its optical signal is modulated through the intensity of the signal without conveying any information in phase or frequency. The transmitted signal is real and positive. The visible light communication networks consist of a transmitter, propagation channel, and receiver. The light emitting diode lamp is an appropriate transmitter used for both illumination and communication purposes. The photodetector is used as a receiver. It is a diode device, which is sensitive to the light intensity that can convert the received light into a current modulated by the intensity of the received light. The space located between the light-emitting diode and the photodetector is considered as a propagation channel.

Nowadays, visible light communication becomes a promising technology complementary to RF spectrum roughly (3kHz -300 GHz), which operates in the visible light spectrum band roughly (400 THz -780 THz) for future indoor networking available bandwidth of visible light is 10,000 times larger than that of the microwave RF band [50]. Radio Frequency spectrum resources are limited and need national regulation and authorizations for usage purpose. The rapid growth of wireless communication applications and demand make the radio frequency spectrum to be crowded. To alleviate such spectrum shortage in the radio frequency band, we need to take advantage of the ubiquitous capacity of the visible light spectrum as a viable solution.

The basic limitation of visible light communication is that the narrow bandwidth modulation of LEDs. Additionally, data transmission rate decreases with increasing of distance between transmitter and receiver. Multiple-Input Multiple-Output is used in radio frequency-based communi-

cation to provide higher data rates. As in RF communication, in order to increase data rate VLC uses multiple LEDs as transmitters and multiple photodetectors as receiver. Non-Orthogonal Multiple Access enables multiple users to utilize the similar spectrum resource simultaneously by applying interference cancellation at the receiver. Therefore, it is very important to apply MIMO systems in VLC networks to obtain high data rates and apply NOMA systems to make users to utilize entire bandwidth.

1.2   Statement of the Problem

Visible light communication networks have emerged as a possible option for data access, primarily for indoor environments in recent years. Practically, VLC networks are realized by using the light-emitting diodes as the transmitters. However, developing a high data rate in the visible light communication system is difficult due to the narrow modulation bandwidth of the light-emitting diode. Furthermore, the data rate achieved by employing OFDMA in the VLC system is reduced due to spectrum partitioning. On the other hand, applying power domain NOMA to MIMO-VLC networks can achieve high data rates using the entire available modulation bandwidth of LEDs. However, the conventional power allocation approach GRPA and NGDPA can't improve the performance of edge users. Therefore, it is crucial to analyze and enhance the performance of MIMO-NOMA-based VLC networks by developing and investigating better power allocation strategies that can improve achievable data rates.

1.3   Significance of the Study

In the last decades, the rapid increase in data traffic exposes the limitation of using only radio frequency-based mobile communications whose spectrum becomes congested and scarce. Several technologies have been studied and developed to solve such spectrum congestion problems. Furthermore, advances in LED technologies make visible light communication systems supplement RF-based communication systems. However, due to the small bandwidth modulation of LEDs achieving a high data rate is problematic. By applying power domain NOMA to MIMO-VLC, we can achieve a high data rate. But, a better power allocation approach is essential to improve the performance of edge users. This study will enhance the performance of edge users by proposing new power splitting techniques in MIMO-NOMA-based VLC networks.

1.4 Objectives of the Study

1.4.1 General Objectives

To analyze and enhance the performance of downlink MIMO-NOMA-based visible light communication systems.

1.4.2 Specific Objectives

- To analyze the sum rate of Non-Orthogonal Multiple Access in downlink MIMO visible light communication system.

- To compute the achievable rate of the far user and the near user.

- To compare the sum rate gain achieved by different power allocation techniques of NOMA in visible light communication networks.

- To propose a new power splitting approach that improves the performance of edge users.

1.5 Methodology

Firstly, different research reports, journal articles, and other published and unpublished documents are reviewed regarding power domain non-orthogonal multiple access and MIMO-based visible light communication systems. The appropriate power allocation scheme of NOMA is crucial to VLC networks. In the power domain NOMA, fair power allocation plays a vital role in enhancing visible light communication networks. Secondly, a new power splitting scheme that exploits user channel conditions was proposed to improve the performance of edge users. Performance metrics like sum rate, average sum rate, and sum-rate gain of proposed NOMA and other conventional power allocation schemes NGDPA and GRPA are studied. Finally, the performance of those power allocation schemes in indoor MIMO-based visible light communication networks was analyzed and validated using Matlab software.

1.6 Scope and Delimitation of the Study

The primary intention of this thesis was to concentrate on analyzing and enhancing the performance of MIMO-based visible light communication systems through integrating with the power

domain NOMA in indoor downlink communications. A new power splitting scheme of NOMA that can enhance the performance of edge users was proposed and analyzed. The performance of the proposed NOMA, GRPA, and NGDPA was investigated and compared with each other. Additionally, the study had covered the following points:

- Studying the main limitations of LED used for both illumination and data transmission.

- Studying the impact of MIMO techniques in a visible light communication system.

- Integrating power domain NOMA with visible light communication technology.

Delimitations of the study were:

- Only a downlink indoor communication system is considered.

- In visible light communication systems, LEDs are fixed on the ceiling for data transmission in indoor communication. In such communication system, user mobility is not significant. Therefore, the impact of user mobility is not considered.

- Due to characteristics of visible communication channels, only line-of-sight is taken into consideration.

1.7 Thesis Organization

The rest of this thesis is organized in the following manner. Chapter 2 is a literature study that explains a detailed background for visible light communication and revises the related literature and studies on MIMO-NOMA-based VLC systems. Chapter 3 gives a brief overview of optical wireless communication, visible light communication, IEEE standards for visible light communication, comparisons between optical wireless communication, visible light communication and radio frequency technologies, MIMO application in VLC system, and essential features of non-orthogonal multiple access, and its principles. Chapter 4 discusses the overall system model of downlink MIMO-NOMA-based Visible Light Communication Systems. Chapter 5 describes the simulation scenarios, results, and detailed discussions. Finally, Chapter 6 concludes the thesis and puts some recommendations as a future direction.

CHAPTER 2

2   Review of Related Literature

2.1   Related Literature

Visible Light Communications was conceived in Japan [10, 11], and there is increasing interest in Europe, including work in a European Commission Framework 7 project OMEGA [12]. Standardization work is also underway within the IEEE. The lighting industry increasingly employs white LED devices for illumination and signaling applications. It is thought that such solid-state lighting will eventually replace existing conventional lighting sources due to their reliability and predicted high efficiency. Such sources can also be modulated to provide simultaneous illumination and communication.

The critical components of visible light communications are the light-emitting diode, photodiode, physical layer (PHY), and media access control (MAC). The light-emitting diode changes an electrical signal to optical energy that gives illumination as well as communication. Information is line encoded and modulated by the PHY and then conveyed on the optical signal by modulating the amplitude or some other feature of the LED light. At the receiver, the photodetector changes the received optical power into an electrical signal, and then it is demodulated and decoded by the PHY layer to recover the user message bits. The MAC is the second layer in the Open Systems Interconnection seven-layer models to support a color packet scheme and media access control, depending on the applications [12].

Developing large capacity visible light communication system is difficult due to the small modulation bandwidth of light-emitting diodes. To solve such problems, different kinds of literature have been proposed various techniques to boost the capacity of visible light communication systems. Some of them are discussed below.

Applying the MIMO methods accomplishes a high data rates in VLC [13]. Achieving a high data rate is challenging due to the low modulation bandwidth of the sources (several MHz), but the illumination levels specified for occupation ensure that a very high signal-to-noise ratio

is available. The availability of many high signal-to-noise ratio channels with low bandwidth makes MIMO techniques an appealing option for achieving high data rates.

Orthogonal frequency division multiple access (OFDMA) has been applied in VLC systems [14]. It has been shown that proposed OFDMA based VLC system can effectively use the bandwidth of the available LED sources. However, the achievable data rate by employing OFDMA is reduced due to the spectrum partitioning.

In [15], the design principles, key features, benefits, and weaknesses of existing dominant NOMA schemes are examined and compared. In conventional orthogonal multiple access (OMA) schemes, multiple users are allocated with radio resources that are orthogonal in time, frequency or code domain. Theoretically, it is understandable that OMA cannot always accomplish the sum-rate capacity of multi-user wireless systems [10]. Aside from that, in conventional OMA schemes, the maximum number of supported users is restricted by the total amount and the scheduling granularity of orthogonal resources.

Non-orthogonal multiple accesses via power domain multiplexing have been proposed for 5G systems due to their superior spectral efficiency [14]. NOMA allows multiple users to share time and frequency resources in the same spatial layer via power domain or code domain multiplexing.

In [16], it has been shown that NOMA performs much better in high signal-to-noise ratio scenarios. Visible Light Communication systems need high signal to noise ratios due to the short distance between the transmitter and the receiver. From this fact, it is beneficial to apply NOMA in downlink VLC systems.

In [17]-[20], the performance of NOMA-based VLC has been investigated. In [18], NOMA is suggested as a potential candidate for high-speed visible light communication systems and furthermore a gain ratio power allocation method is proposed. More advanced power allocation techniques for NOMA-based visible light communication systems were proposed in [19], however, with relatively high computational complexity. In [20], a phase pre- distortion approach was proposed to improve the error rate performance of uplink NOMA-based visible light com-

munication systems.

In [20], the author proposes MIMO techniques to increase system capacity and extend indoor visible light communications coverage. In [21], a MIMO-NOMA-based VLC system was experimentally verified. The authors experimentally investigated a system with a single carrier mode of transmission, using the frequency domain successive interference cancelation, but without considering the power allocation problem. When applying MIMO, the power allocation method of the single LED NOMA-VLC systems cannot be directly adopted in MIMO-NOMA-based VLC systems.

Most recently, in paper [22], the author proposed a power allocation algorithm called normalized gain difference power allocation approach aimed at reducing the complexity and increasing the efficiency of 2×2 MIMO-NOMA-VLC systems with multiple users.The author applied NGDPA techniques for a low number of users. Only two (2) and three (3) users are considered, which is not practically applicable.

To the best of my knowledge, it is essential to have better power allocation techniques which can improve performance of edge user. As the number of users increases in indoor visible light communication systems, the performance of NGDPA and GRPA will decrease. Along these lines, to improve the performance of edge users, a new power allocation strategy is proposed for a larger number of users in the considered area.

CHAPTER 3

3 Overview on Optical Wireless Communication

3.1 Optical Wireless Communication

Nowadays, better data rate capacity is required to address the demand for extensive volume mobile data. The upcoming wireless generations (5G and 6G) provide several new and additional services with massive connectivity, ultra-large system capacity, low latency, and ultra-minimal energy consumption. There is a great challenge on future 5G and beyond wireless communication systems to address the higher volume data rate demand. Hence, the rapid mobile user data demand increment needs an efficient solution to guarantee and satisfy their quality of services. Radio frequency communication-based networking is well established and becomes more congested and restricted since they have limited spectrum size. Due to such problems, many scholars currently study and find out different investigations on license-free Electro-Magnetic (EM) spectrums (especially on the optical spectrum) to support the exponentially growing data rate demands. Light-emitting diode-based optical wireless communication becomes a promising candidate for such high data rate demand.

Optical wireless communication uses visible light spectrum as a propagation medium, and it provides efficient networking features such as higher energy efficiency, better security, and EM interference-free. Using OWC, we can achieve up to 100 Gbps data rate in standard indoor communication and illumination levels. Moreover, optical wireless communication technologies provide and support energy-efficient communication, and most of these technologies require easy implementation with small infrastructure [25]-[27]. There are different optical wireless communication technologies that realize the wireless communication data delivery. Those technologies are light fidelity and visible light communication.

Optical wireless communication uses visible light, infrared radiation, or ultraviolet spectra as a communication media [28]-[31]. Figure 3.1 shows different application platforms of optical wireless communication. All of those communication technologies, such as user-to-

machine/device, device-to-device, machine-to-machine, vehicle to- vehicle, point-to-point, point-to-multipoint, and multipoint-to-point, need higher data rates [32].

Several optical wireless communication systems are designed and developed with different optical bands. Some of those OWC technologies are: visible light communication, light fidelity, free-space optical communication, and optical camera communication. The communication protocol, application scenario, architecture, and propagation media for these optical wireless communication technologies are different. Fundamental limitations of optical communication systems are: highly dependence on the line-of-sight (LOS), sensitivity to small blockages, limited coverage area, outdoor atmosphere degrades the system performance and corrupted by different light sources interference's.
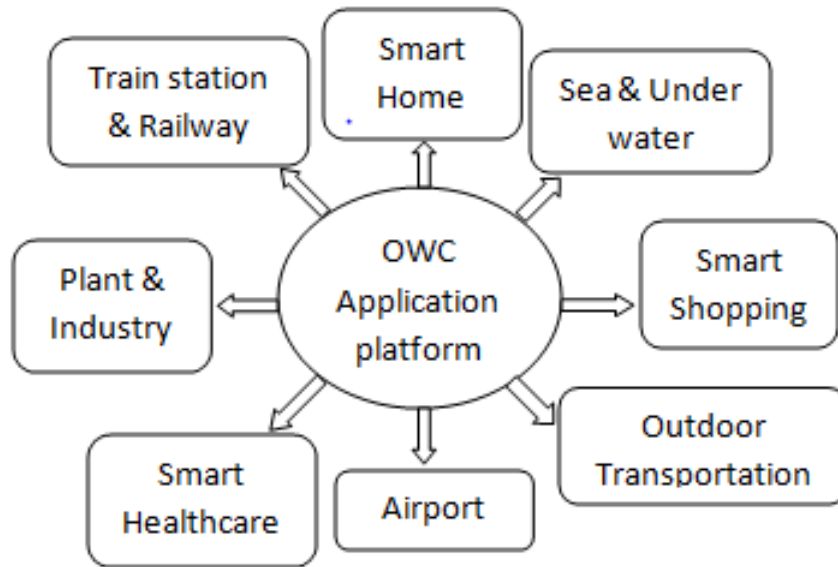
Figure 3.1: Application platforms of OWC[32].

In the early stage of wireless generations, mobile phones were used only for voice communication and text messaging. However, a new era of mobile technologies started after the introduction of iPhone smartphones by 2007. Nowadays, smart mobile phones are used for multi-purpose applications to provide video chatting, health monitoring, cloud services, online streaming, and so on. To support and provide such a higher data rate required unlimited users need, we need to allocate large bandwidth. However, there is no free spectrum on the current radio frequency range to support such complete user data rate requirements. This problem led

researchers to investigate new communication technologies to fully address user's need with higher data rates and low costs.

Table 3.1: Comparison of different optical wireless communication technologies [29].

Issue	*VLC*	*Li-Fi*	*FSO*
Transmitter	LED or LD	LED or LD	LD
Receiver	PD or camera	PD	PD
Data Rate	• 10 Gbps using LED • 100 Gbps using LD	• 10 Gbps using LED • 100 Gbps using LD	40 Gbps
Comm. Distance	20 m	10 m	> 10,000 km
Spectrum	VL	IR/VL/UV	IR/VL/UV
Mobility Support	Not mandatory	Mandatory	No
Advantages	• Wide spectrum • Support both comm. and illumination • High security	• Point-to-multipoint comm. • Wide spectrum • High security	• Bidirectional comm. • Support long range comm. • High security
Limitations	• Mobility support not guaranteed • Small coverage area • Poor performance in outdoor applications • Affected by external condition	• Small coverage area • Poor performance in outdoor applications • Limited to NLOS comm.	• Affected by fog, snow and dust • Only support LOS comm.

Due to dramatically growing broadband mobile subscriber numbers (which is expected, by 2022 around 9.4 billion) [2] and the emergence of the Internet of Technology (IoT), the growth of the demand for traffic becomes unprecedented. So that, future wireless network generations should satisfy such change by addressing related technical challenges for minimizing data transmis-

sion latency and improving spectral efficiency. The main directions of the ongoing, visible light technology research efforts are:

- Investigating the potential capacities of the unlicensed IR spectrum (300 GHz–430 THz) and VL spectrum (430 THz–790 THz).

- Improving the available radio frequency spectrum efficiency by finding and adopting advanced multiple access schemes and new modulation techniques. In this respect, visible light communication has an emerged and promising technology for small cell wireless networking.

3.2   Visible Light Communication

Visible light communication is emerging as a promising candidate means to overcome the crowded RF spectrum for highly localized communication systems. It supports data communication and illumination in indoor environments where new energy-efficient light-emitting diode materials and devices will replace old incandescent and fluorescent lighting. According to reports, indoor environment data's demand is higher than the outdoor environment. This is because 80% of the whole time, people were staying in an indoor environment. Such phenomena make visible light communication the most attractive and a promising candidate for future wireless technologies [33].

Visible light communication is a subset of optical wireless communication technologies in which data exchanges use visible light and widely uses commercial light-emitting diodes as a transmitter. Visible light communication is a fusion network technology between wireless communication and light-emitting diode illumination. Wireless technologies are designed for efficient data rate transmission, higher security, and higher reliability. Light-emitting diode technologies are designed and fabricated as a power-efficient device with long-life lighting technology.

Visible light communication provides new services through developed light-emitting diode light sources. We can use visible light-based wireless communication within a restricted environment because visible light-based wireless communication systems do not interfere with any

electric equipment that has a restricted frequency spectrum. Light-emitting diode-based intelligent transportation technologies can provide and gives specific information to man or vehicles to guide drivers for safe driving. Every application and service of a visible light communication system support reliability and security since light cannot travel through buildings and walls.

The main challenge of visible light communication systems was that they were corrupted by external light sources like computer screens or the sun. Such light sources degrade the signal-to-noise ratio of visible light communication networks. To minimize such impact, we need to carefully design and install the communication system, including the optical concentrators, directionality and lenses, electrical signal processing, and optical filtering. Another challenge on visible light communication is finding the best modulation strategy suitable for different kinds of visible light communication applications. To enable high data rate transmission, we need to use off-the-shelf standard LEDs, and apply intensity modulation with direct detection (IM/DD) to realize the modulation and demodulation process. Since visible lights cannot penetrate through walls and objects, we can easily install them in small cells and achieves high-quality accesses with minimum inter-cell interference.

One of the main drawbacks of VLC systems is that the modulation bandwidth of VLC access points (LEDs) is limited and restricts users' achievable data rate. To use the benefits of VLC systems fully, we need to use and study further advanced multiple access schemes, multiple input multiple output, and optical modulation techniques [34]. Critical features of visible light communications are:
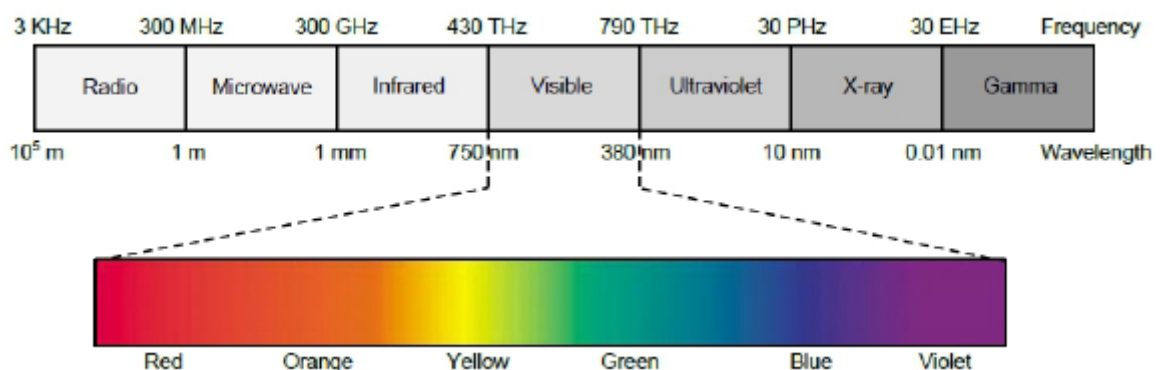

Figure 3.2: VL frequency range on Electromagnetic Spectrum[48].

- *Low cost*: The VLC system implementation is relatively simple. Instead of planning and designing the hole wireless communication system, we can reuse the ubiquitous lighting infrastructure by adding few additional modules to the existing lighting system.

- *Big capacity and spatial reuse*: VLC working frequency is in the order of terahertz. Hence, it provides a bigger capacity than that of RF spectrum communication.

- *Immune to electromagnetic interference*: Low interference from existing RF communication technology due to the VLC working in unlicensed spectrum.

- *Easy implementation*: Since VLC modules can make small and compact size, we can easily implement and install into the existing lighting infrastructure. The digital to analog converter, modulation unit, and driving circuit can be integrated into LEDs.

- *Enhance security*: Unlike RF signals, light cannot pass through walls, and thus the chance of eavesdropping is virtually nonexistent.

- *Energy Efficient and Cost-Effective*: The transmitter (LED) needs minimum level energy for processing. Only a few upgrades of existing lighting infrastructure are required rather than the initial set up cost of an entire communication system. LEDs are easily controllable, and energy-efficient light sources roughly use one-twentieth of conventional light source energy.

- *Provide supplementary service*: Because VLC uses LED as a transmitter, VLC gives lighting service while providing communication service.

Visible light communication technologies are new communication technologies in which signals are transported through modulated visible light beams. Such systems take advantage of LEDs that can be pulsed at very high speeds without noticeable impact on the lighting output and the human eye. Visible light communication can be applicable in various applications, including wireless personal area networks, wireless local area networks, and vehicular networks. Visible light communication channel characteristics are different from any other wireless communication technologies, including RF communication. In VLC systems, the optical input signal is modulated through signal intensity without carrying information in frequency or phase,

the optical signal power is proportional to the input signal power (not square of the amplitude of the signal), the transmitted optical signal is real and positive, the peak power of the transmitted optical signal is constrained by the illumination requirements and the dynamic range of LEDs.

Visible light-based wireless communication poses several challenges. Among such problems, dimming support and flicker mitigation are some of the main challenges. Dimming support is a problem related to energy efficiency and power saving challenges in visible light communication. To minimize such issues, we need to address an arbitrary dimming demand of visible light communication users as a light source. The fluctuation of light brightness (flickering) is another crucial issue in visible light communication. Since flicker causes harmful/negative and noticeable physiological or behavioral changes in humans, we need to potentially mitigate any flickers resulting from the light source modulation of communication. To avoid such fluctuation problems, we need to use the maximum period. The optimal and accepted period is greater than 200 Hz (maximum period < 5 *ms*), which is safe [36]. As a result, we can remove any noticeable flickering occurrence during the VLC modulation process by applying such a maximum period.

3.3 Standards of Visible Light Communication

Functioning of visible light communication standalone system is regulated by IEEE 802.15.7 standard for interoperable visible light-based communication systems. By 2009, the Task Group of IEEE 802.15.7 Visible Light Communication develops a PHY and MAC standard for visible light communications. The standards developed by the task group define a PHY and MAC layer for short-range OWC using visible light. The spectral wavelength for visible light extends from 380 *nm* to 780 *nm*.

The standard is liable of delivering sufficient data rates for supporting video and audio multimedia services and also considers the mobility of the visible data link, compatibility with VL infrastructures, impairments due to interference and noise (from ambient light and other environmental effects), and a media access control layer that accommodates VL links. Its basic potential applications are: secure point-to-point communication, secure point-to-multipoint communication (office, airplane, hospital), and indoor location-based service. IEEE 802.15.7
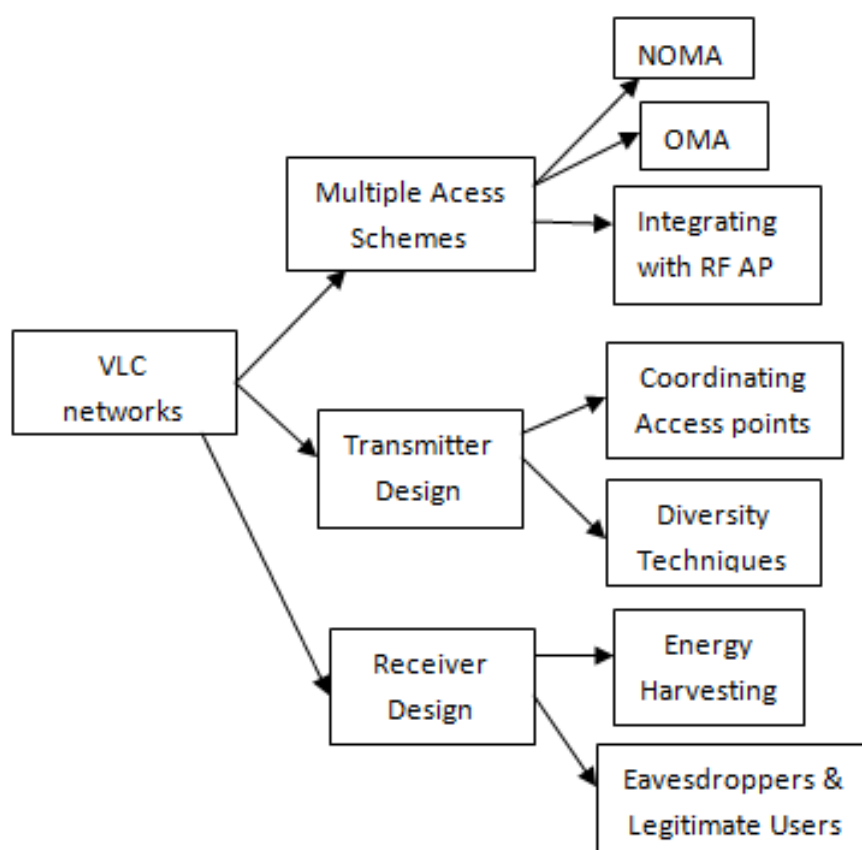
Figure 3.3: Visible light communication networks [29].

VLC standard further defines and divides the PHY layer for different applications. Those defined physical layers are explained below.

1. *PHY I*: Such standard envisioned for the outdoor environment with minimum data rate applications, and it uses on-off keying and variable pulse position modulation with data rates in the range from tens to hundreds of kbps.

2. *PHY II*: Such standard envisioned for indoor environment with moderate data rate applications, and it uses on-off keying and variable pulse position modulation with data rates in the tens of Mbps.

3. *PHY III*: Such standard envisioned for applications that have multiple light sources with detectors, and it uses color shift keying with data rates in the tens of Mbps.

PHY I standard also provides Reed Solomon and convolutional coding for error correction since it is designed for short frames with minimum data rates. *PHY II* and *PHY III* support only Reed

Table 3.2: IEEE 802.15.7 VLC standard summary [39].

Entity	*Characteristics*	*Entity*	*Characteristics*
Addressing	• 16 - bit • 64 - bit	Device Classification	• Infrastructure • Mobile • Vehicle
MAC Supported Topology	• Star • P2P • Broadcast	Clock Rate Selection	• Multiple on the range 200 kHz to 120 MHz
Collision Avoidance Scheme	• Slotted random access with collision avoidance • Scheduled	MAC Specifications	• Color Function • Visibility • Dimming • Visual Indication • Device Security • Reliable Link • Mobility
Modulation Scheme	• OOK • VPPM • CSK	Contention Period	• Contention Free Period • Contention Access Period
Acknowledgment	• Yes	Multiple Channel Usage	• Supported

Solomon coding. *PHY I* and *PHY II* also support a run-length limited code to provide clock recovery, DC balance, and flicker mitigation. In addition to coding and modulation, different optical rates are provided for all physical layer types to support a broad class of optical transmitters (LEDs) for various applications [12].

A new working group (called IEEE 802.15.7r1) formed in 2014 revised the previous visible light communication standards [38]-[40]. This group specifies three main application scenarios related to different data capacities and communication devices. Those scenarios are:

I. *Light Emitting Diode Identification (LED-ID)*: A low data rate photodiode-based commu-

nication sends identification signals through multiple LEDs.

II. *Optical Camera Communication (OCC)*: Which is an image-sensor-based communication that offers localization and message broadcasting. Accordingly, there are three source types specified, those are: surface source (on the range of 90 bps - 8 kbps), discrete source (on the range of 15 bps- 4 kbps), and 2D screen source (on the range of 40 bps - 64 kbps).

III. *Light Fidelity (LiFi)*: Which is a photodiode-based communication that supports high data rate streams in the order of Gbps, handover, mobility, and bidirectional multiple access. Its technical specifications are focusing on coding, bandwidth, optical clock rate, and modulation.

Generally, the primary purpose of such visible light communication standard is that to put a global guideline for short-distance optical wireless communication for providing services on several unlicensed bands.

3.4   MIMO Visible Light Communication

The capability of LED used as a transmitter will facilitate the design and implementation of optical MIMO for visible light communication. As in RF-MIMO systems, optical MIMO uses multiple LEDs to improve the performance of visible light communication systems. This performance is enhancement achieved when transmitters with multiple LEDs are used in conjunction with receivers with multiple photo detectors. Therefore, performance enhancement comes about the utilization of spatial multiplexing, which increases the systems throughput or spatial diversity, decreasing the bit error rate (BER) [47]. The spectral efficiency is enhanced due to the establishment of a parallel communication platform. But, spatial multiplexing for optical MIMO is not an an effective technique for improving the data transmission rates for non-imaging receivers [13].

The design and implementation of optical MIMO for VLC systems are not easy due to limited spatial diversity compared to RF-MIMO systems [48]. This issue is predominant in indoor applications where the paths taken by the transmitted signals from the transmitter to the receiver are diverse as opposed to naturally various paths in RF MIMO systems. The design of optical

MIMO system receiver is designed as either non-imaging or imaging receiver. For a non-imaging receiver, a group of the photodetector is arranged without any independence on each other, and each of them has their optical concentrator [47]. This kind of receiver is essential for high gain, which can be provided due to the narrow field of view of individual photo detectors. In imaging receivers, the image sensors are employed as constituents of the receiver.

3.5 Non-Orthogonal Multiple Access

In a non-orthogonal multiple access schemes, users are multiplexed in the power-domain or code domain (CD). In PD non-orthogonal multiple access, users are multiplexed in the power domain by assigning distinct power levels to different users, while CD non-orthogonal multiple access utilizes user-specific spreading sequences to multiplex the users in the code domain, such as the well-known code division multiple access techniques [35]. The Power domain non-orthogonal multiple accesses uses superposition coding on the transmitter side and successive interference cancellation at the receivers. Its basic principles are; the receiver detects one signal from the received composite signal while treating other signals present in the same composite signal as noise. Then, the detected signal is subtracted from the received composite signal to detect the other signals. If we assume that a user experience a deep fading with poorer channel gain, applying conventional orthogonal multiple access is inefficient, since the bandwidth allocated to such user is wasted. But by using NOMA, the bandwidth is allocated to other users; hence the bandwidth efficiency is improved significantly [41]. The key features of non-orthogonal multiple access schemes are as follows [42].

- *Utilization of the power domain for user multiplexing*: In NOMA, the power domain, which has not been used for multiple access in conventional cellular networks, is used for user multiplexing.

- *Utilization of different channel conditions*: In contrast to conventional OMA schemes, the diverse channel conditions among users are utilized in the NOMA scheme. Let us take a scenario with a single antenna node as an example. The power allocation coefficients, which are the combination coefficients for superposition coding, are determined by the user's channel conditions. Specifically, a message for a user with a strong channel gain is

allocated less transmission power, and a message for a user with poor channel conditions allocates more power.

Currently, all the wireless cellular network systems are implemented with orthogonal multiple access techniques. However, none of these OMA techniques can meet the high user data demands of future cellular network systems. In TDMA, the signal for each user is sent in non-overlapping time slots, and accurate timing synchronization becomes challenging, especially in the uplink transmission. In FDMA, signals for every user are appointed to a subset of subcarriers, and CDMA performs codes to isolate the users over a similar channel. Non-orthogonal multiple access is essentially different from these multiple access schemes, which provide orthogonal access to the users either in time, frequency, code, or space, and each user operates in the same band where they are distinguished by their power levels.

3.6 Principles of Non-Orthogonal Multiple Access

The primary and valuable principle of non-orthogonal multiple access is to enhance spectrum sharing between end-users, instead of allocating them to fixed orthogonal blocks. If we apply power domain non-orthogonal multiple access, the user signals first superimposed by the access point and broadcast such mixed signals to the whole users, and hence all users are allocated and served at the same time/frequency/code with distinct power levels. These different power level allocations are decided through power allocation coefficients. Since non-orthogonal multiple access ensures to serve all users with better rate fairness, we need to use an efficient power allocation strategy. As a result, such power domain non-orthogonal multiple access allocates more power level for users who have poorer channel gain conditions than users with better channel conditions [43, 44]. Assigning more power for users who have stronger channel conditions may enhance the throughput, but it may disconnect poorer channel condition users from the network. At the receiving end, there are different detection policies based on the user's channel conditions.

In a PD non-orthogonal multiple access based network, strongest channel condition users decode and filter out their partner's signal first and then decode their messages through a well-known procedure called successive interference cancellation. On the other hand, poorer users

treat others signal as noise and then decode their message directly, which is logical since the poorer channel condition user's information was transmitted at a higher power level than the rest users [45]. The main reason behind applying successive interference cancellation for users with stronger channel conditions in PD non-orthogonal multiple access-based networks is that their own signals were buried below their partner's signal during superimposed signals transmitted from the access points. To provide the same spectrum for all users, we need to apply super-position coding at the transmitter side and successive interference cancellation at the receiver side. The transmitter should split the power between the user signal waveforms and superimpose them accurately. This method of downlink power splitting strategy is different for uplink channels.
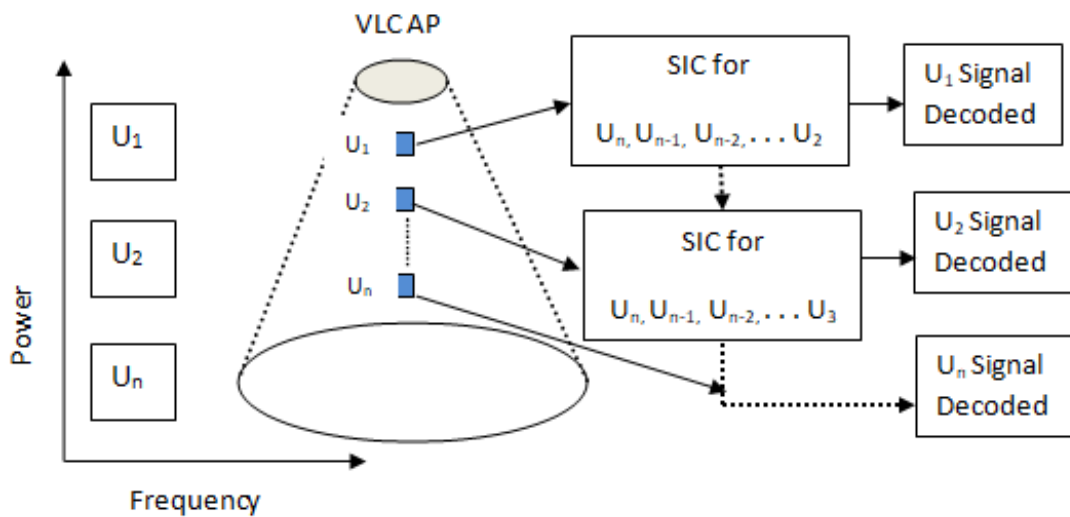
Figure 3.4: PD multiplexing for *N* users downlink NOMA [45].

CHAPTER 4

4 System Model

4.1 System Model

In this study, the downlink of an indoor MIMO-NOMA-based Visible Light Communication network with multiple LEDs simultaneously serving K users was considered. Assume that the LED transmitter is installed on the ceiling, which has i down confronting LEDs and communicates with K users; every user has j up confronting photo-detectors. As done in [22], the 2×2 MIMO-VLC has been extended to the 4×4 MIMO-VLC networks. Therefore, without loss of generality, assume that there are four LEDs $(i = 1, 2, 3, 4)$ on the ceiling serving K number of users and each user is equipped with four PDs $(j = 1, 2, 3, 4)$. The parameters of all LEDs and PDs are assumed to be identical. Therefore, the system considered represents a typical MIMO Visible Light Communication system model. Multiple PDs are equipped with each NOMA user who can utilize the entire available modulation bandwidth of LEDs. The block diagram of such a system is shown below in figure 4.1.

Figure 4.1: System Block Diagram.

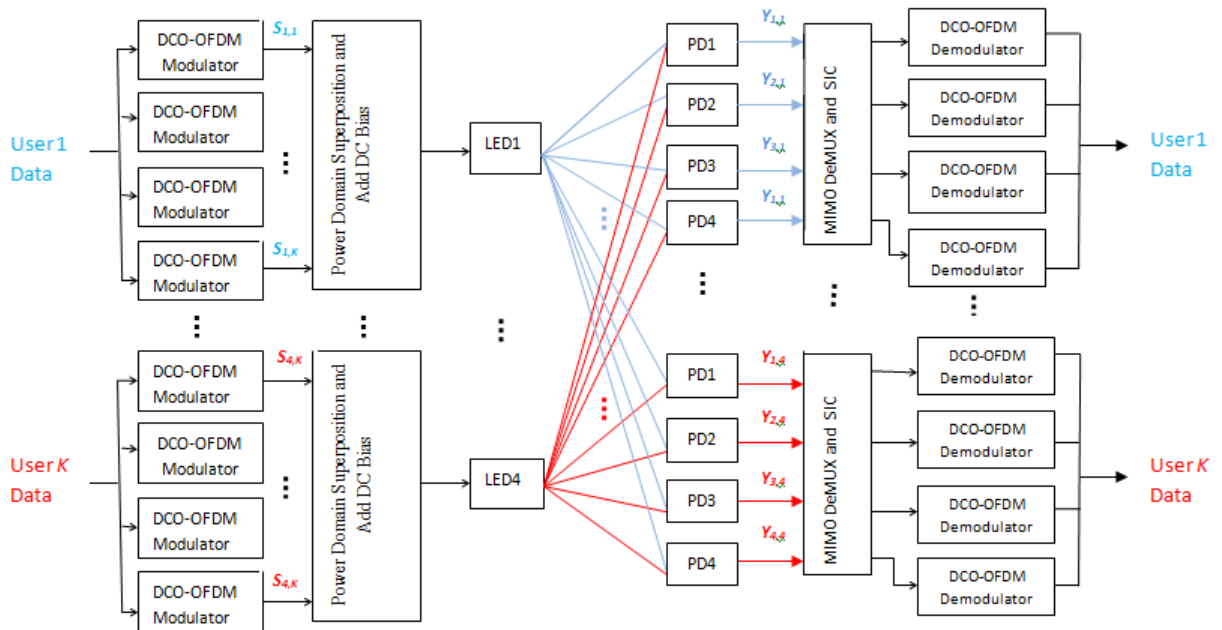According to power domain multiplexing NOMA principle, the ith transmitter LED simultaneously transmits the message data s_i to all K users by using all the bandwidth through a superposition coding technique at the transmitter side.

4.2 DC-biased optical OFDM Modulation

Orthogonal Frequency Division Multiplexing is broadly considered a modulation technique for the Intensity Modulated/Direct Detection optical wireless system because of its capacity to transform the entire bandwidth channel into smaller sub-channels, each with a flat response within their sub-band. It can avoid Inter Symbol Interference (ISI) and subsequently provides resistance to the dispersive channels. OFDM is proposed for Optical Wireless Communication in the ITU-T g.9991 (g.vlc), the IEEE 802.15.7m and the IEEE 802.11bb, and other standards [37].

In the Intensity Modulated/Direct Detection optical system, light intensity can neither be complex nor negative. Therefore, the input feeding the Inverse Fast Fourier Transform (IFFT) during the OFDM generation flow is constrained to have a Hermitian symmetry to deliver a real-valued signal. A DC bias is usually applied to ensure a positive output, called DC-biased Optical OFDM (DC-OFDM) [49].

In this study, the downlink MIMO-NOMA-based Visible Light Communication 4 QAM-based DC biased optical OFDM modulation was considered. After DC biasing optical OFDM modulation, the transmitted signal of the ith LED is the combination signals of K users, which can be expressed as [22]:

$$x_{i,k} = \sum_{k=1}^{K} \sqrt{\rho_{i,k}} s_{i,k}(t) + I_{DC} \tag{4.1}$$

Where $s_{i,k}(t)$ is the modulated message signal intended for the $k^{th}(k = 1,2,...,K)$ user from the ith LED, $\rho_{i,k}$ is the electrical power allocated for the kth user in the ith LED, and I_{DC} is the DC bias provided to each LED to ensure that the instantaneous transmitted signal remains to be positive.

4.3 LOS Propagation Channel Model for VLC

The summed-up Lambertian radiation pattern model was applied to find the LED's line-of-sight irradiance. The geometric model of LOS transmission is shown in figure 4.2. As compared to non-line-of-sight (NLOS), the line-of-sight provides much higher intensity of light in visible light communication system [13]. Therefore, in this study only line-of-sight transmission was taken into consideration. The line-of-sight channel gain of the optical link between the ith LED and the jth PD of the kth user is given by [18, 22]:
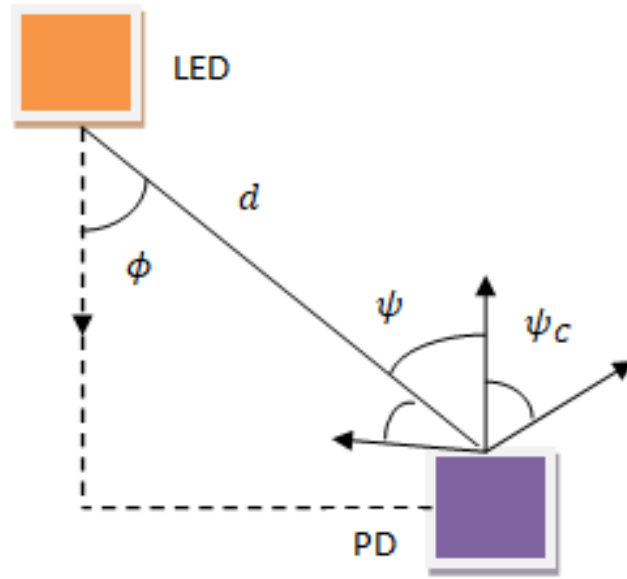
Figure 4.2: Geometric model of LOS transmission.

$$h_{ji,k} = \begin{cases} \frac{(m+1)A_{PD}}{2\pi d^2} T_s(\psi)g(\psi)\cos^m(\phi)\cos(\psi), & 0 \leq \psi \leq \psi_c \\ 0, & \psi > \psi_c \end{cases} \tag{4.2}$$

$$m = -\frac{\ln 2}{\ln(\cos(\Phi_{1/2}))} \tag{4.3}$$

Where d is the LOS distance between the ith LED and the jth PD of the kth user, m is the Lambertian emission order and $\Phi_{1/2}$ is the semi angle at half power of the LED, A_{PD} is an active area of PD, ϕ is the transmitter viewing angle (also referred to as irradiation angle), ψ is the angle of incidence with respect to the receiver axis, ψ_c is the concentrator field of view (FOV),

n is the internal refractive index of the concentrator, $T_s(\psi)$ denotes the gain of the optical filter adopted at the receiver and $g(\psi)$ represents the gain of the non-imaging concentrator, which is given by [17]:

$$g(\psi) = \begin{cases} \frac{n^2}{\sin^2(\psi_c)}, & 0 \leq \psi \leq \psi_c \\ 0, & \psi > \psi_c \end{cases} \tag{4.4}$$

After going through a free-space optical wireless channel, the optical intensity signal is converted at the PD receivers of the kth user into a current signal via photo-electric conversion, and further, the constant DC-offset I_{DC} is removed in the electrical domain. In general, noise is assumed to be introduced in the electrical domain. After transmission, the electrical signal received at the jth PD of the kth user is expressed as:

$$y_{j,k} = \mu \Re P_{opt} \sum_{i=1}^{4} h_{ji,k} x_i(t) + n_{j,k} \tag{4.5}$$

Where $\Re$ is responsivity of PD, P_{opt} is optical output power, μ is modulation index, $n_{j,k}$ is the Additive Gaussian Noise with zero mean and variance $\sigma_{j,k}^2$. It is composed of thermal noise and shot noise. The received electrical signal of kth user can be expressed in matrix form as [22, 23, 24]:

$$Y_k = \mu \Re P_{opt} H_k X + N_k \tag{4.6}$$

Where $X = [x_1 x_2 x_3 x_4]^T$ is transmitted electrical signal vector, H_k is channel gain matrix and N_k is Additive White Noise vector. The channel gain matrix can be given as:

$$H_k = \begin{bmatrix} h_{11} & h_{12} & h_{13} & h_{14} \\ h_{21} & h_{22} & h_{23} & h_{24} \\ h_{31} & h_{32} & h_{33} & h_{34} \\ h_{41} & h_{42} & h_{43} & h_{44} \end{bmatrix} \tag{4.7}$$

4.4 Zero Forcing (ZF) MIMO Receiver

Zero Forcing detection is a simple and viable technique for recovering multiple data streams at the receiver. But it needs knowledge of channel state information. In this study, ZF-MIMO

de-multiplexing was used to retrieve the transmitted data with primary channel inversion due to its low complexity [51]. The normalized estimated electrical signal vector at the output of the ZF-MIMO receiver of the kth user is given as [23]:

$$\tilde{X}_k = \frac{1}{\mu \Re P_{opt}} Y_k N_k = X + \frac{1}{\mu \Re P_{opt}} \hat{H}_k N_k \tag{4.8}$$

Where $\hat{H}_k \triangleq \left(H_k^T H_k\right)^{-1} H_k^T$ is the is the pseudo inverse of H_k and $(.)^T$ denotes transpose operation. In Visible Light Communication channels, the diversity gain is severely limited because of the high correlation between signal paths; hence conventional MIMO-VLC systems are symmetric (i.e., It is 4×4 in this case). Therefore, the pseudo inverse is simplified to $\hat{H}_k \triangleq H_k^{-1}$ and the above equation (4.8) is reduced to [22, 23]:

$$\tilde{X}_k = X + \frac{1}{\mu \Re P_{opt}} W_k \tag{4.9}$$

Where $W_k \triangleq H_k^{-1} N_k$. As the results, the estimated signal received by k^{th} user from i^{th} LED is [24]:

$$\tilde{x}_{i,k}(t) = \sum_{k=1}^{K} \sqrt{\rho_{i,k}} s_{i,k}(t) + \frac{1}{\mu \Re P_{opt}} w_{i,k} + I_{DC} \tag{4.10}$$

Where $w_{i,k}$ is the ith element of the vector W_k. From the above equation (4.10), the researcher has observed that the estimated signal contains a message signal from all users. In order to extract the desired message signal, successive interference cancellation is applied at the receiver. To apply SIC, the decoding order of the users must be determined for every LED. Sorting the users is done by finding the optical channel's sum of every user for every LED. Without loss of generality, it is assumed that K users for the ith LED are sorted in descending order of their sum optical channel gains as follows:

$$h_{1i,1} + h_{2i,1} + h_{3i,1} + h_{4i,1} > h_{1i,2} + h_{2i,2} + h_{3i,2} + h_{4i,2} > ... > h_{1i,K} + h_{2i,K} + h_{3i,K} + h_{4i,K} \tag{4.11}$$

With reference to the ith LED, the decoding order is then set to be [22]

$$O_{i,1} < O_{i,2} < ... < O_{i,K} \tag{4.12}$$

Finally, at k^{th} user, the estimated message signal from i^{th} LED can be expressed as [24]:

$$\tilde{s}_{i,k}(t) = \sqrt{\rho_{i,k}} s_{i,k}(t) + \sum_{k=k+1}^{K} \sqrt{\rho_{i,k}} s_{i,k}(t) + \frac{1}{\mu \Re P_{opt}} w_{i,k} \tag{4.13}$$

.

4.5 Power Allocation Strategy

Due to the difficulty of achieving higher throughput and minimizing the fairness problem among end users, optimal power allocation is critical in non-orthogonal multiple access systems. Different power allocation strategies have been proposed for VLC networks. Some of them are: fixed power allocation (FPA), gain ratio power allocation, normalized gain difference power allocation. The main target behind these different power allocation strategies are:

- Since the minimum power level is enough to decode signals for good channel condition users, we need to assign a small fraction of power for those users.

- Allocating a large fraction of power for bad channel condition users to filter out and decode their information's from the superimposed signal.

4.5.1 Gain Ratio Power Allocation (GRPA)

In the power domain NOMA, a gain ratio power allocation scheme, which considers user channel conditions to guarantee equal and efficient allocation, can boost the overall device performance [34]. Because of its simplicity and effectiveness, GRPA has been proposed as a power allocation for many NOMA-based VLC systems. In the GRPA techniques, optical power depends upon any optical channel of the device. Specifically, for the GRPA approach proposed in [15], the power allocation technique is determined by the optical channel gains of users compared to the gain of the first sorted user. According to decoding order in the equation (4.12), the relationship between electrical powers allocated to user k and $(k+1)$ following the ith LED is given as [22, 15]:

$$\rho_{i,k} = \left(\frac{h_{1i,k+1} + h_{2i,k+1} + h_{3i,k+1} + h_{4i,k+1}}{h_{1i,1} + h_{2i,1} + h_{3i,1} + h_{4i,1}} \right)^{k+1} \rho_{i,k+1} \qquad (4.14)$$

4.5.2 Normalized Gain Difference Power Allocation (NGDPA)

In order to improve the achievable sum rate of NOMA-based MIMO-VLC networks, an efficient power allocation approach called Normalized Gain Difference Power Allocation is proposed in [22] . In NGDPA, the optical channel gain difference is used to allocate power. According to the decoding order presented in the equation (4.12), the relationship between electrical powers

assigned to user k and $(k+1)$ by the ith LED is described as [22]:

$$\rho_{i,k} = \left(\frac{h_{1i,k} + h_{2i,k} + h_{3i,k} + h_{4i,k} - h_{1i,k+1} - h_{2i,k+1} - h_{3i,k+1} - h_{4i,k+1}}{h_{1i,1} + h_{2i,1} + h_{3i,1} + h_{4i,1}} \right)^k \rho_{i,k+1} \quad (4.15)$$

4.5.3 Proposed Power Allocation

In this study, a new power splitting strategy is proposed to enhance the power allocation efficiency among end-users. Based on the channel gain order presented in the equation (4.12), the relationship between electrical powers allocated to user k and $(k+1)$ in accordance with the ith LED is given in the following relationship.

$$\rho_{i,k} = \left(\frac{h_{1i,1} + h_{2i,1} + h_{3i,1} + h_{4i,1}}{h_{1i,1} + h_{2i,1} + h_{3i,1} + h_{4i,1} + h_{1i,k+1} + h_{2i,k+1} + h_{3i,k+1} + h_{4i,k+1}} \right)^k \rho_{i,k+1} \quad (4.16)$$

To maintain overall electrical power for the ith transmitter LED to be constant, the power allocation should satisfy the following constraint [22].

$$\sum_{k=1}^{K} \rho_{i,k} = Pe = 1 \quad (4.17)$$

Where Pe is total electrical power. When applying SIC decoding at the receiver, the users with lower decoding order should handle higher values of interference and also encounter poorer channel conditions. Therefore, to ensure fairness among users, the users with lower decoding order are allocated higher power. The relationship between power allocated to successive users for $(k > 1)$ is given by:

$$\rho_{i,k} = \alpha_{i,k} \rho_{i,k-1} \quad (4.18)$$

Where $0 \leq \alpha_{i,k} \leq 1$ is the power allocation coefficient of the kth user at the ith LED. Thus, depending up on the above constraint in equation (4.17), the power allocated to the first user $(k = 1)$ is given by:

$$\rho_{i,1} = \frac{Pe}{1 + \sum_{j=2}^{K} \prod_{m=1}^{j-1} \alpha_{i,m}} \quad (4.19)$$

From (4.18) and (4.19) equations, power allocated to the kth user $(k > 1)$ can be generalized as:

$$\rho_{i,k} = \frac{Pe \prod_{m=1}^{k-1} \alpha_{i,m}}{1 + \sum_{j=2}^{K} \prod_{m=1}^{j-1} \alpha_{i,m}} \quad (4.20)$$

4.6   Signal to Noise Ratio and Achievable Sum Rate

4.6.1   Signal to Noise Ratio

The Signal to Noise Ratio is a parameter defining the strength of the signal carrying the information and comparing it to that of an unwanted signal. In the visible light communication system, since the noise vector is composed of the shot noise and the thermal noise, it is expected that the total noise is dominated by the White Gaussian component [52]. Shot noise is mainly generated by LED lights and the ambient light in the PIN tube. Thermal noise is generated by the amplifier and loaded into the receiver. It is primarily caused by free electrons or charge carriers inside the resistor for irregular thermal motion. The noise generated has Gaussian distribution of zero mean and variance of [52]:

$$\sigma_{nk}^2 = \sigma_{sh}^2 + \sigma_{th}^2 \tag{4.21}$$

Where σ_{nk}^2 is total noise variances, σ_{sh}^2 is shot noise variances and σ_{th}^2 is thermal noise variances. The shot noise variances at k^{th} user is determined by [51, 52]:

$$\sigma_{sh}^2 = 2 \times q \times \left(\Re \times P_{rx} + I_{bg} \times I_2 \right) \times Bw \tag{4.22}$$

Where q is the electronic charge, $\Re$ is the photodetector responsivity, P_{rx} is the received optical power for k^{th} user, Bw is the equivalent bandwidth, I_{bg} is the photocurrent due to background radiation and I_2 is the noise bandwidth factor. The thermal noise variances at k^{th} user is determined by [51]:

$$\sigma_{th}^2 = 8 \times \pi \times K \times T \times \eta \times A_{PD} \times B^2 \times \left(\frac{I_2}{G} + 2 \times \pi \times \gamma \times \eta \times A_{PD} \times I_3 \times \frac{Bw}{g_m} \right) \tag{4.23}$$

Where K is Boltzmann constant, T is Temperature in Kelvin, G is Open-loop Voltage Gain, η is Fixed Capacitance, γ is Field Effect Transistor (FET) channel noise factor and g_m is FET Transconductor. Signal to Noise Ratio is determined as follows [25]:

$$SNR_{i,k} = \frac{(\Re P_{rx})^2}{\sigma_{nk}^2} \tag{4.24}$$

4.6.2 Achievable Sum Rate

The sum rate of 4×4 MIMO-VLC system of K user is given by:

$$SR_K = Re\left(\sum_{k=1}^{K} \sum_{i=1}^{4} \frac{\frac{Bw}{2} \log_2 (1 + SNR_{i,k})}{10^6} \right) \tag{4.25}$$

Where Bw is the transmission bandwidth, $SNR_{i,k}$ is the signal-to-noise ratio for each link between the ith LED and the kth user. Re operator is to evaluate the real part. That means the equation output only contains real values, not imaginary values.

4.6.3 Achievable Rate

The achievable data rate of kth user get from all i^{th} LED is determined as follows:

$$R_k = Re\left(\sum_{i=1}^{4} \frac{\frac{Bw}{2} \log_2 (1 + SNR_{i,k})}{10^6} \right) \tag{4.26}$$

4.6.4 Sumrate Gain

The following equation gives sum rate gain of proposed NOMA over NGDPA and GRPA.

$$SR\,gain_{NOMA/NGDPA} = \left(\frac{SR_{NOMA/Proposed} - SR_{NOMA/NGDPA}}{SR_{NOMA/NGDPA}} \right) \times 100 \tag{4.27}$$

Where $SR\,gain_{NOMA/NGDPA}$ is sum-rate gain of proposed NOMA over NGDPA, $SR_{NOMA/Proposed}$ is sum-rate of proposed NOMA and $SR_{NOMA/NGDPA}$ is sum-rate of NGDPA.

$$SR\,gain_{NOMA/GRPA} = \left(\frac{SR_{NOMA/Proposed} - SR_{NOMA/GRPA}}{SR_{NOMA/GRPA}} \right) \times 100 \tag{4.28}$$

Where $SR\,gain_{NOMA/GRPA}$ is sum-rate gain of proposed NOMA over GRPA, $SR_{NOMA/Proposed}$ is sum-rate of proposed NOMA and $SR_{NOMA/GRPA}$ is sum-rate of GRPA.

CHAPTER 5

5   Simulation Results and Discussions

5.1   Simulation Scenario

The performance of the total sum rate, sum rate gain, and achievable rate of different power allocation techniques for NOMA-based MIMO-VLC system were analyzed. In the simulations, the system is set up as four LED on the ceiling used as transmitter, and each user are equipped with four PD inside a typical room as shown figure 5.1 . The normalized offset has been defined for system coverage. The distance from user one $(k = 1)$, which has the largest channel gain sum, to the user K, which has the smallest channel gain sum, is fixed as $r(m)$. The maximum distance from the user $(k = 1)$ to the edge of the system is $R(m)$. All users are uniformly distributed over system coverage. The normalized offset of user K with respect to the user $(k = 1)$ is defined as $\frac{r}{R}$, and the normalized offset of user k with respect to the user $(k = 1)$ is defined as $\frac{(k-1)r}{(K-1)R}$. The parameters used during simulation analysis are given in table 5.1.
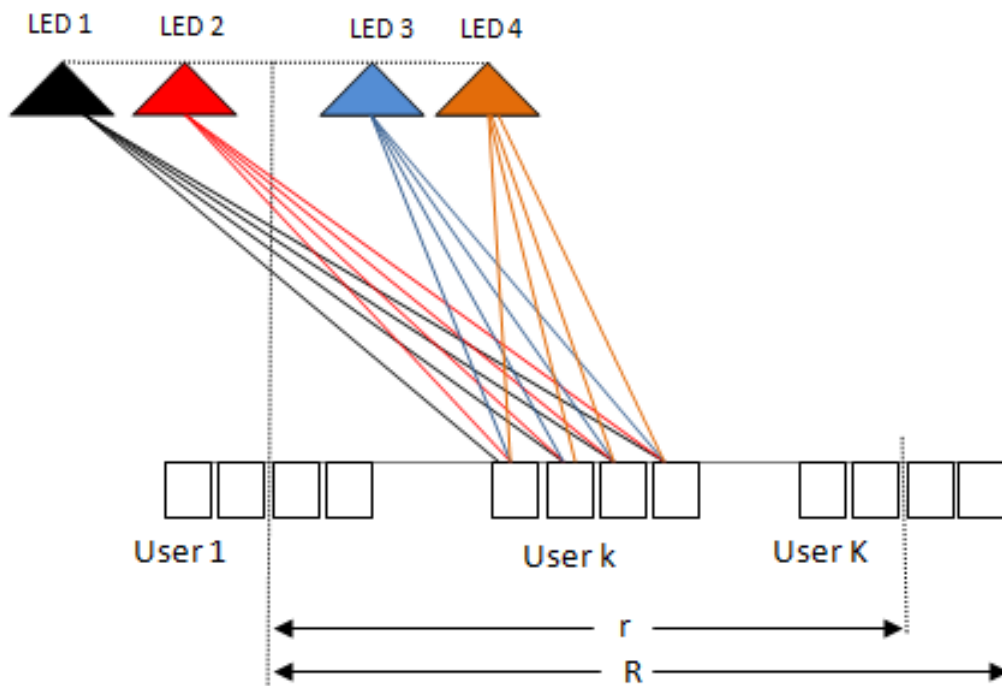

Figure 5.1: Illustration of a 4×4 MIMO-NOMA based VLC system with K users.

Table 5.1: System and channel model parameters.

Simulation Setup	Value
Number of LEDs	4
System Coverage	$0.2 - 4m$ (Variable)
Number of User	$2 - 10$ (Variable)
Receiver height	$0.85m$

(a) Simulation setup

Transmitter parameter	Value
Transmitted power	10 W
Modulation index	0.5
Transmitter semi angle	$60°$
Separation between LED	$1m$

(b) Transmitter Parameter

Noise parameter	Value
Electronic charge	$1.6 \times e^{-19}C$
Noise bandwidth factor	0.562
Boltzmann constant	$1.38 \times e^{-23}$
Absolute temprature	$300K$
Fixed capacitance	$112e^{-12}/1e^{-4}(F/m)$
Open loop voltage gain	10
FET transconductance	$30e^{-3}S$
FET channel noise factor	1.5

(c) Noise Parameter

Reciever parameter	Value
Receiver field of view	$72°$
Total bandwidth	10 MHz
Photodiode responsivity	0.53 A/W
Refractive index	1.5
Separation between PD	$4cm$
Gain of optical filter	0.9
Physical area of a PD	$1\ cm^2$

(d) Reciever Parameter

5.2 Results and Discussions

5.2.1 Power Allocation Coefficient

Table 5.2 shows how power is allocated from LED 1 by using GRPA, NGDPA, and proposed NOMA techniques for five users in the considered system coverage. The power allocation coefficient is calculated according to constraint explained in equation (4.17).

Table 5.2: Power Allocation Coefficient for five users from LED 1

|	*Power Allocation Coefficient*		
User No	*GRPA*	*NGDPA*	*Proposed NOMA*
1	$2.4415 \times e^{-7}$	0.0050	0.0288
2	$4.3278 \times e^{-7}$	0.0201	0.0505
3	$3.4052 \times e^{-6}$	0.0815	0.1140
4	$3.2713 \times e^{-4}$	0.2587	0.2619
5	0.9996	0.6345	0.5447

5.2.2 Sum rate of Proposed NOMA vs. OFDMA

According to the simulation setup and simulation parameter given above, to validate the effectiveness of the proposed NOMA, Orthogonal Frequency Multiple Access has been taken into consideration. Figure 5.2a shows the performance superiority of the proposed NOMA over OFDMA for three users ($k = 3$) uniformly distributed in a coverage area. It has been clear that the sum-rate utilized by OFDMA is decreased continuously as normalized offset value increases. For example, the user located at the border of the system obtained 187 Mbit/s by employing OFDMA. However, by using the proposed NOMA, the user at the border got 266.4 Mbit/s. At the edge of system coverage, the user utilized a sum rate of 253.1 Mbit/s and 222 Mbit/s by applying NGDPA and GRPA, respectively. Generally, the proposed NOMA has superior performance than OFDMA and even than the other conventional power allocation.

Figure 5.2b illustrates sum rate utilized by proposed NOMA, NGDPA, GRPA, and OFDMA for five users ($k = 5$). Sum rate achieved by GRPA decreased significanltly for $0.5 \leq r/R \leq 1$. Also, sum rate obtained by OFDMA declined continuously. Here again, proposed NOMA performed better than the other techniques.

Figure 5.2c shows the achievable sum rate utilized by proposed NOMA, NGDPA, GRPA, and OFDMA for six users ($k = 6$). The proposed NOMA and NGDPA achieved a sum rate of 261.9

Mbit/s and 235.3 Mbit/s at the border of system coverage. The OFDMA utilized a sum rate of 198.9 Mbit/s while GRPA achieved a sum rate of 152.3 Mbit/s at the system's edge.
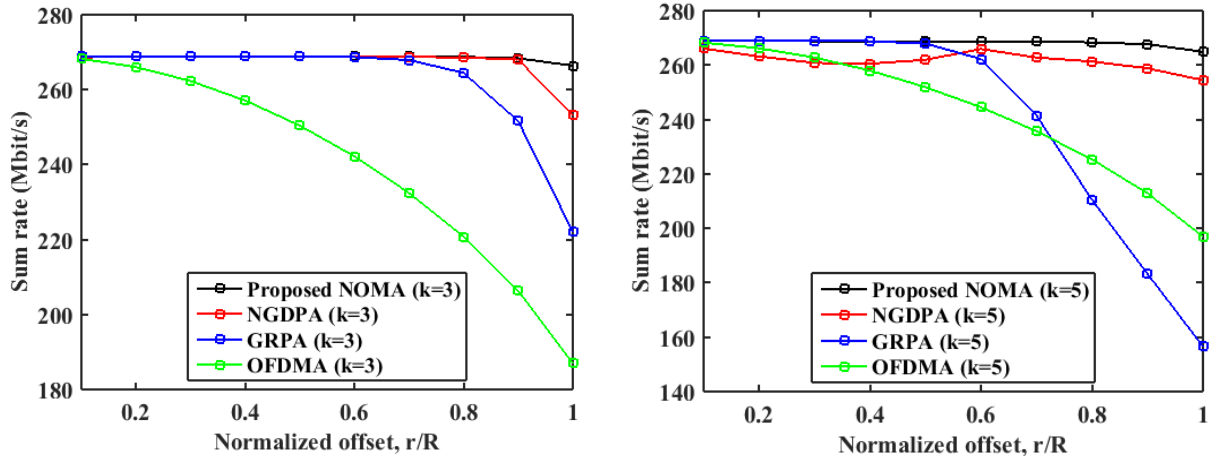
(a) Achievable Sum rate of Proposed NOMA over NGDPA, GRPA and OFDMA vs. r/R ($k = 3$)

(b) Achievable Sum rate of Proposed NOMA over NGDPA, GRPA and OFDMA vs. r/R ($k = 5$)
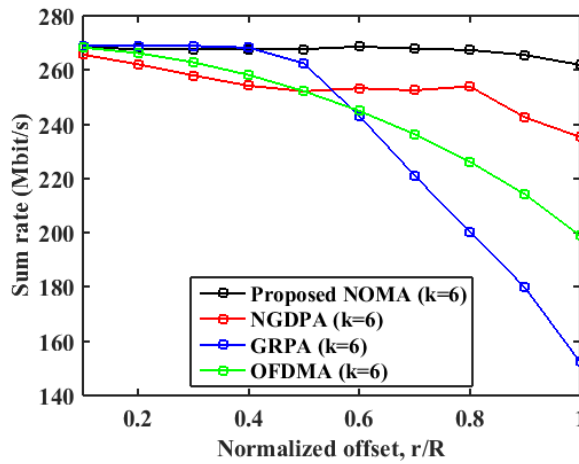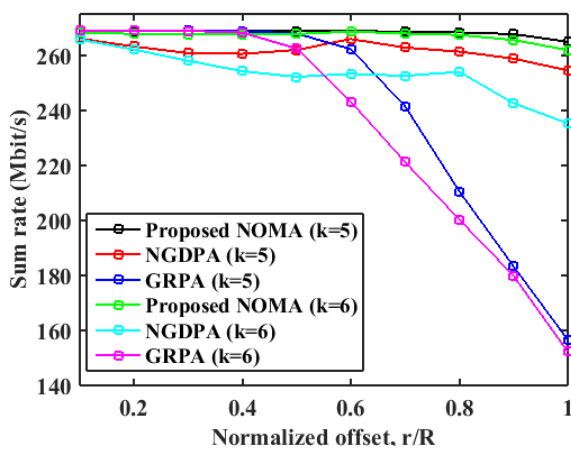
(c) Achievable Sum rate of Proposed NOMA over NGDPA, GRPA and OFDMA vs. r/R ($k = 6$)
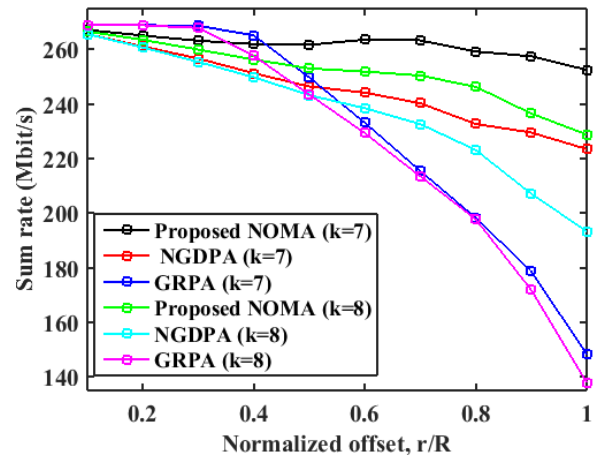
Figure 5.2: Achievable Sum rate of Proposed NOMA over NGDPA, GRPA and OFDMA vs. Normalized offset

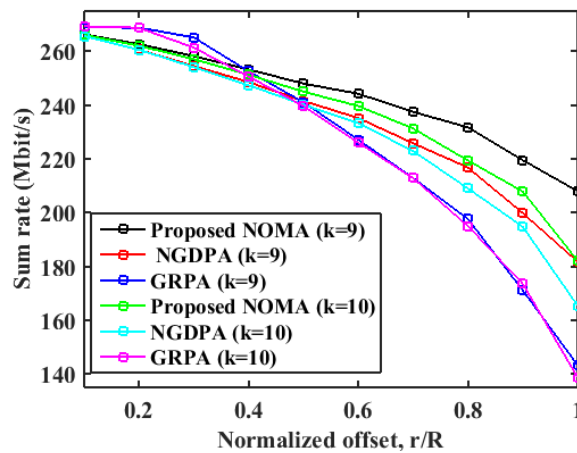### 5.2.3 Achievable Sum Rate vs. Normalized Offset

The achievable sum rate of different users has been simulated by using parameter given in the table 5.1 according to geometric setup defined in figure 5.1.

(a) Achievable Sum rate of Proposed NOMA over NGDPA and GRPA vs. r/R ($k = 5, 6$)

(b) Achievable Sum rate of Proposed NOMA over NGDPA and GRPA vs. r/R ($k = 7, 8$)

(c) Achievable Sum rate of Proposed NOMA over NGDPA and GRPA vs. r/R ($k = 9, 10$)

Figure 5.3: Achievable Sum rate of Proposed NOMA over NGDPA and GRPA vs. Normalized offset

Figure 5.3a shows the achievable sum rate of proposed NOMA, NGDPA, and GRPA versus normalized offset for user five ($k = 5$) and user six ($k = 6$). In both cases, proposed NOMA utilizes a higher sum rate. The proposed NOMA achieves a sum rate of 264.89 Mbit/s and 261.89 Mbit/s for ($k = 5$) and ($k = 6$), respectively at the edge of the system. NGDPA achieves a sum rate of 254.45 Mbit/s and 235.28 Mbit/s for ($k = 5$) and ($k = 6$), respectively at the edge of the system. GRPA achieves a sum rate of 156.59 Mbit/s and 152.27 Mbits/s for ($k = 5$) and ($k = 6$), respectively at the edge of the system.

Table 5.3: Achievable sum-rate comparison of proposed NOMA, NGDPA, and GRPA (k=7 & k=8).

	Achievable Sum rate (Mbit/s)					
r/R	*GRPA (k=7)*	*GRPA (k=8)*	*NGDPA (k=7)*	*NGDPA (k=8)*	*Proposed NOMA (k=7)*	*Proposed NOMA (k=8)*
0.1	268.94	268.94	265.67	265.65	267.17	266.64
0.2	268.93	268.90	261.12	260.72	265.11	263.54
0.3	268.70	267.90	256.69	255.48	263.23	259.97
0.4	265.18	257.68	251.31	249.83	261.10	256.33
0.5	249.74	243.48	246.44	243.28	261.70	253.07
0.6	233.17	229.36	244.18	238.47	263.63	251.90
0.7	215.52	213.52	240.32	232.66	263.38	250.45
0.8	198.26	197.79	232.71	223.17	259.27	246.34
0.9	178.72	171.84	229.57	207.13	257.53	236.53
1	148.30	137.88	223.49	193.36	252.55	228.85

Figure 5.3b illustrates the achievable sum rate of proposed NOMA, NGDPA, and GRPA versus normalized offset for seven ($k = 7$) and eight ($k = 8$) users. In both cases, proposed NOMA utilizes a higher sum rate. The proposed NOMA achieves a sum rate of 252.55 Mbit/s and 228.85 Mbit/s for ($k = 7$) and ($k = 8$) respectively at the edge of the system. NGDPA achieves a sum rate of 223.49 Mbit/s and 193.36 Mbit/s for ($k = 7$) and ($k = 8$) respectively at the edge of the system. GRPA achieves a sum rate of 148.30 Mbit/s and 137.88 Mbits/s for ($k = 7$) and ($k = 8$) respectively at the edge of the system.

Figure 5.3c shows the achievable sum rate of proposed NOMA, NGDPA, and GRPA versus normalized offset for nine ($k = 9$) and ten ($k = 10$) users. In both cases, proposed NOMA utilizes a higher sum rate. The proposed NOMA achieves a sum rate of 208.03 Mbit/s and

182.19 Mbit/s for $(k = 9)$ and $(k = 10)$ respectively at the edge of the system. NGDPA achieves a sum rate of 181.80 Mbit/s and 165.44 Mbit/s for $(k = 9)$ and $(k = 10)$ respectively at the edge of the system. GRPA achieves a sum rate of 143.34 Mbit/s and 138.77 Mbits/s for $(k = 9)$ and $(k = 10)$ respectively at the edge of the system.

Table 5.4: Achievable sum rate comparison of proposed NOMA, NGDPA and GRPA (k=9 & k=10).

	Achievable Sum rate (Mbit/s)					
r/R	*GRPA (k=9)*	*GRPA (k=10)*	*NGDPA (k=9)*	*NGDPA (k=10)*	*Proposed NOMA (k=9)*	*Proposed NOMA (k=10)*
0.1	268.94	269.33	265.65	265.65	266.33	266.15
0.2	268.84	268.78	260.63	260.62	262.68	262.11
0.3	265.18	261.39	254.57	254.15	258.24	257.08
0.4	252.60	250.64	248.57	247.42	253.27	251.32
0.5	241.07	239.67	241.55	240.22	248.04	245.00
0.6	227.17	226.08	235.30	233.26	244.25	239.68
0.7	212.88	212.83	225.83	222.98	237.47	231.33
0.8	197.66	195.04	216.80	209.02	231.76	219.41
0.9	171.13	173.56	199.85	194.82	219.53	207.89
1	143.34	138.77	181.80	165.44	208.03	182.19

Tables 5.3 and 5.4 show a comparison of the achievable sum rates of different user numbers for the proposed NOMA, GRPA, and NGDPA. We can understand that the proposed NOMA is more effective than other power allocation techniques from both tables. Mainly, as normalized offset become increases, the GRPA techniques perform poorly. In addition, the sum rate utilized by NGDPA also becomes lower than the proposed NOMA. Therefore, generally, the proposed NOMA acts more effectively than the other.

From table 5.3 it is understandable that for $0.1 \leq r/R \leq 0.4$, the sum rate utilized by the GRPA approach for user seven ($k = 7$) and eight ($k = 8$) is greater than the sum rate used by the proposed NOMA. However, for $0.5 \leq r/R \leq 1$, the sum rate utilized by GRPA schemes continuously declined. Therefore, it has poor performance at the edge of the system coverage. Also, from table 5.4 for $0.1 \leq r/R \leq 0.3$, GRPA achieved a greater sum-rate than NGDPA and proposed NOMA. Generally, it has been clear that as normalized value increases, the sum rate obtained by both NGDPA and GRPA decreased compared to the proposed NOMA.

5.2.4 Achievable Average Sum Rate vs. User Number

As explained above, ten users are uniformly distributed over system coverage. The average sum rate of different power allocation techniques was calculated over given system coverage *R*.
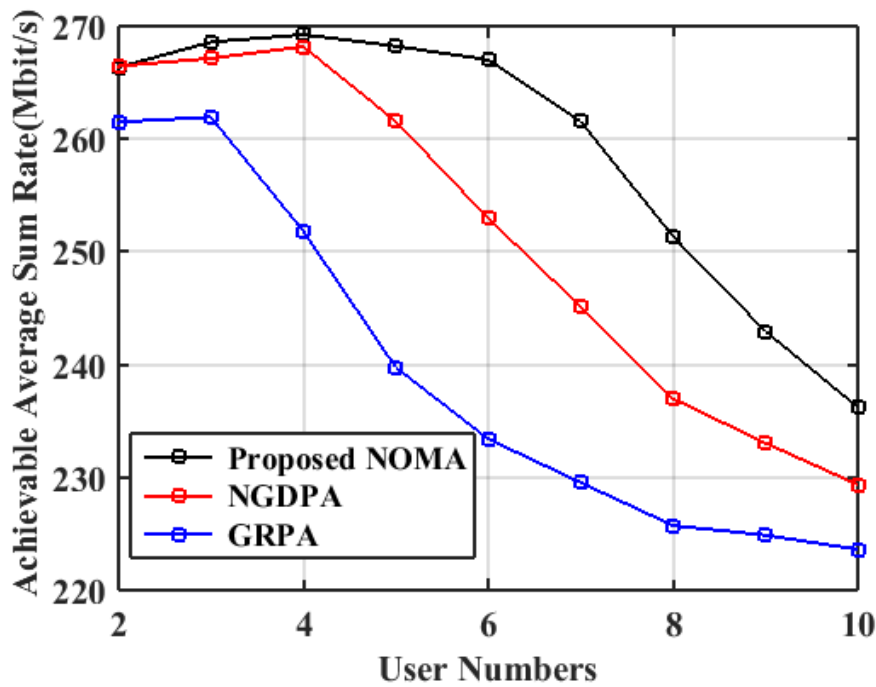

Figure 5.4: Achievable Average Sum Rate vs. User Number

The numerical result shows that as number of users increases in the given area, the total sum rate decreases. When we compare power allocation strategies versus user number, the proposed NOMA improves the average sum rate of edge users as the number of users increases. Specifically, proposed NOMA has the significant improvement of sum rate over GRPA strategies. Especially when a number of a user is greater than four ($k > 4$), the proposed NOMA has

a greater average sum rate than both GRPA and NGDPA, as shown in figure 5.4. Therefore, the proposed NOMA has improved the performance of edge users than the other conventional power allocation techniques GRPA and NGDPA. For six users ($k = 6$), the utilized sum-rate by GRPA declined fastly from 268.2 Mbit/s to 152.3 Mbit/s between $0.4 \leq r/R \leq 1$. However, the sum rate achieved by the proposed NOMA is nearly constant over the entire normalized offset. As a result, the achievable average sum rate utilized by the proposed NOMA is 267 Mbit/s, while the sum rate of GRPA is 233.4 Mbit/s which is a huge difference.
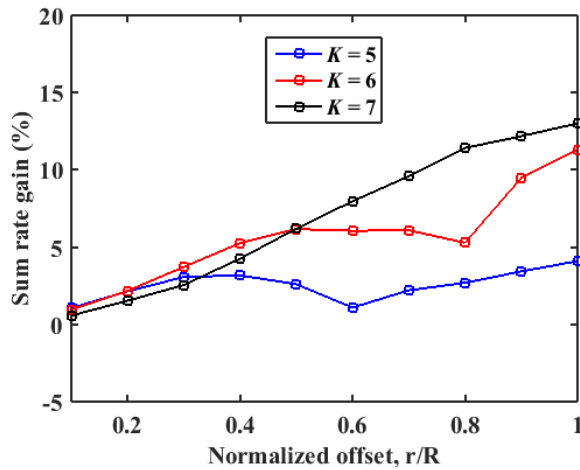
5.2.5   Sum Rate Gain vs. Normalized Offset

Sum rate gain of proposed NOMA over NGDPA and GRPA techniques are analyzed numerically. Figure 5.5a shows sum-rate gain vs. normalized offset of proposed NOMA over NGDPA for user numbers five, six, and seven ($k = 5, 6$, and 7). It has been clear that sum-rate gain increases significantly for large value of the normalized offset. This shows that the performance of edge users is improved. The achievable sum rate gain is 4.097%, 11.31%, and 13% for $k = 5, 6$, and 7, respectively.

Figure 5.5b illustrates sum-rate gain versus normalized offset of proposed NOMA over NGDPA for user numbers eight, nine, and ten ($k = 8, 9$, and 10). The achievable sum rate gain is 18.36%, 14.43%, and 10.12% for $k = 8, 9$, and 10, respectively.

Figure 5.5c shows sum-rate gain vs. normalized offset of proposed NOMA over GRPA for user numbers five, six, and seven ($k = 5, 6$, and 7). The achievable sum rate gain is 69.16%, 71.99%, and 70.3% for $k = 5$, 6, and 7, respectively.
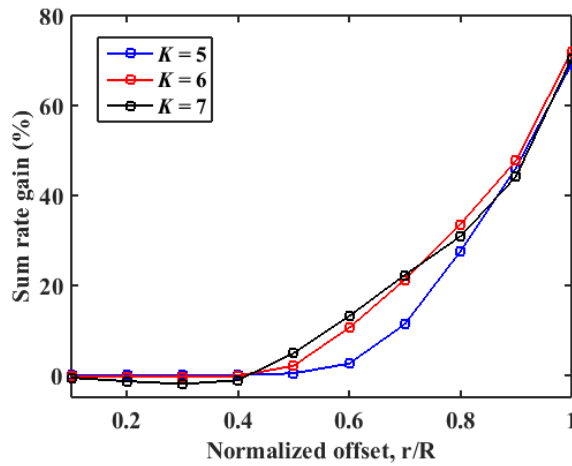
Figure 5.5d shows sum-rate gain vs. normalized offset of proposed NOMA over GRPA for users number eight, nine and ten ($k = 8, 9$ and 10). The achievable sum rate gain is 65.98%, 45.13%, and 31.29% for $k = 8$, 9, and 10, respectively. Generally, we can undestand that lower percentage of sum rate gain for a larger number of users.
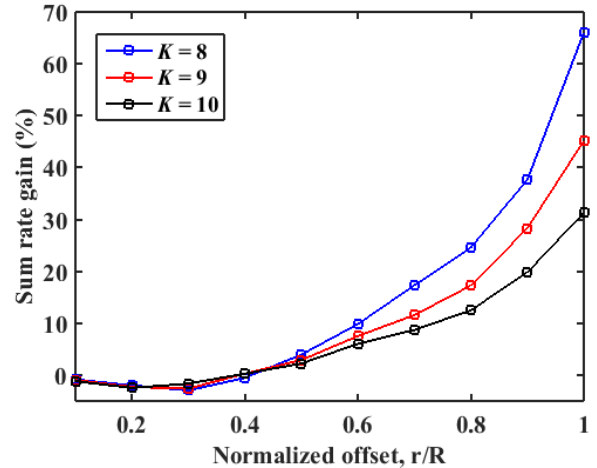
(a) Sum rate gain of Proposed NOMA over NGDPA vs. Normalized offset ($k = 5, 6$ &7)
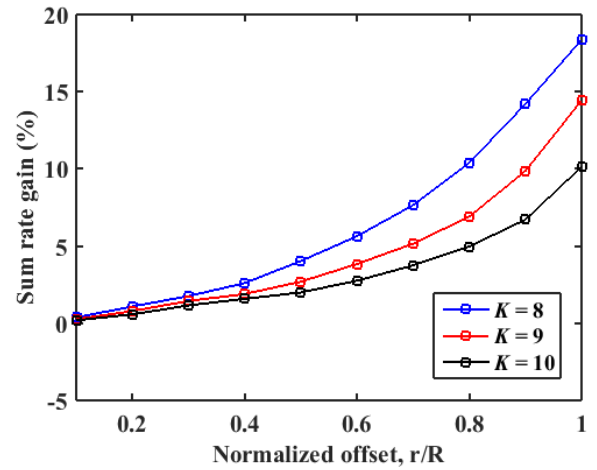
(b) Sum rate gain of Proposed NOMA over NGDPA vs. Normalized offset ($k = 8, 9$ &10)

(c) Sum rate gain of Proposed NOMA over GRPA vs. Normalized offset ($k = 5, 6$ &7)

(d) Sum rate gain of Proposed NOMA over GRPA vs Normalized offset ($k = 8, 9$ &10)

Figure 5.5: Sum rate gain of Proposed NOMA over NGDPA and GRPA vs. Normalized offset

5.2.6 2×2 **MIMO-VLC**

A 2×2 MIMO-VLC has been simulated according to simulation setup in figure 5.1 and simulation parameter given in table 5.1 to show the impact of proposed NOMA over other conventional power allocation strategies of NOMA and OFDMA. The transmitter, receiver, and noise parameters are identical to the 4×4 system except for the number of LEDs and PDs. Figure 5.6a shows the achievable sum rate of proposed NOMA, NGDPA, GRPA, and OFDMA versus normalized offset for four ($k = 4$) users. The proposed NOMA utilized a higher sum rate. The

proposed NOMA, NGDPA, GRPA, and OFDMA achieve a sum rate of 108.17 Mbit/s, 105.88 Mbit/s, 61.63 Mbit/s, and 76.04 Mbit/s, respectively at the system's edge. Here, even if the sum-rate obtained by OFDMA decreased continuously over normalized offset, it can achieve a higher sum rate than GRPA at the border.
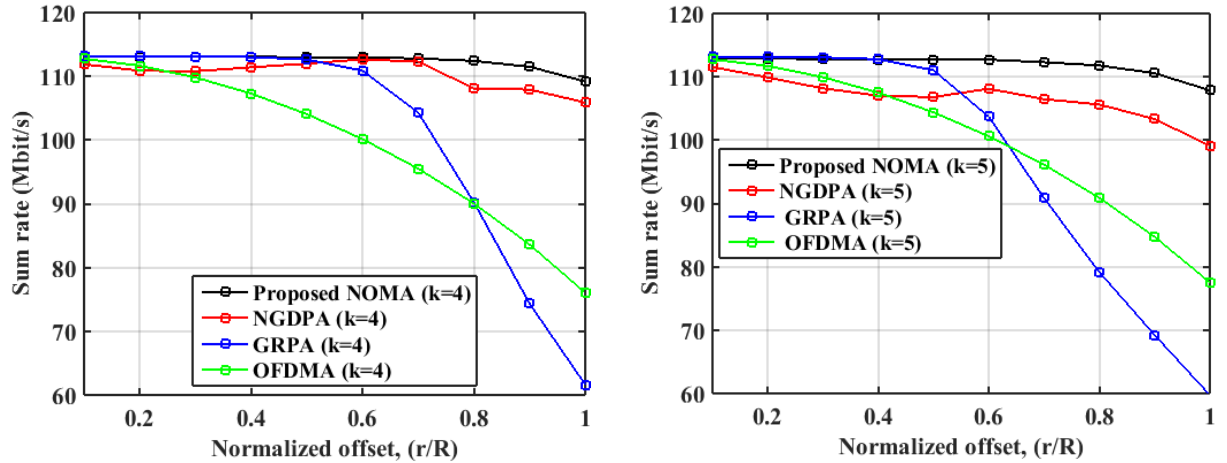
(a) Achievable Sum rate of Proposed NOMA over NGDPA, GRPA and OFDMA vs. r/R ($k = 4$)

(b) Achievable Sum rate of Proposed NOMA over NGDPA, GRPA and OFDMA vs. r/R ($k = 5$)
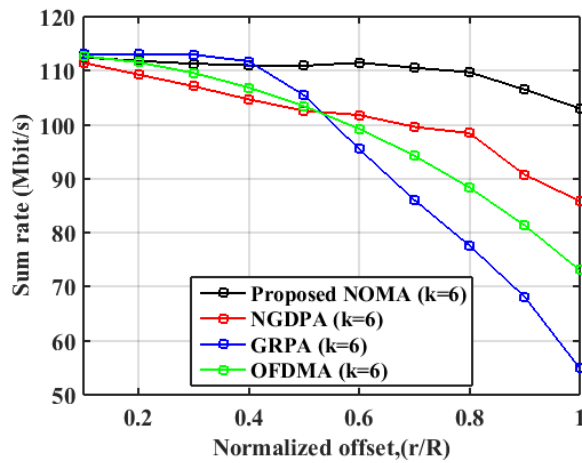
(c) Achievable Sum rate of Proposed NOMA over NGDPA, GRPA and OFDMA vs. r/R ($k = 6$)

Figure 5.6: Achievable Sum rate of Proposed NOMA over NGDPA, GRPA and OFDMA vs. Normalized offset

Figure 5.6b illustrates the achievable sum rate of proposed NOMA, NGDPA, GRPA, and OFDMA versus normalized offset for five ($k = 5$) users. Again, the proposed NOMA achieved a higher sum rate. The proposed NOMA, NGDPA, GRPA, and OFDMA achieved a sum rate of 107.86 Mbit/s, 99.12 Mbit/s, 59.74 Mbit/s, and 77.54 Mbit/s, respectively at the system's border.

Figure 5.6c shows the achievable sum rate of proposed NOMA, NGDPA, GRPA, and OFDMA versus normalized offset for five ($k = 6$) users. Comparing to NGDPA, GRPA, and OFDMA approaches, the proposed NOMA achieved a higher sum rate. For example, the proposed NOMA, NGDPA, GRPA, and OFDMA achieved a sum rate of 103.05 Mbit/s, 85.87 Mbit/s, 54.90 Mbit/s 73.06 Mbit/s, respectively at the system's border.

5.2.7 System Complexity

The overall 4×4 MIMO-NOMA-based VLC is complex because four transmitters and four receivers are in the systems. As a result, there are sixteen possible routes to be evaluated between LEDs and PDs. In addition, the receiver faces complexity as the number of users increased in the coverage area. According to the principle of NOMA, the user with the best channel condition should decode another's signal before decoding his/her signals. As a result, this creates delay and complexity in the overall system.

CHAPTER 6

6   Conclusions and Recommendations

6.1   Conclusions

In this thesis, the performance of a 4×4 downlink MIMO-NOMA-based visible light communication system for a multi user indoor network was studied. The performance was studied through MatLab simulation. Performance metrics like achievable sum rate, sum rate gain, and achievable average sum rate of different users were analyzed. A different power allocation strategy of NOMA in visible light communication systems was considered and compared. In order to enhance the performance of edge users, a new power splitting strategy was also proposed.

The numerical results of simulations show that NOMA will enhance the sum rate of the overall system. Comparison of different power allocation techniques, including GRPA, NGDPA, and proposed NOMA, shows that among the three methods, newly proposed NOMA utilized a higher sum rate for a higher number of users. The proposed NOMA, NGDPA, and GRPA achieved a sum rate of 261.89 Mbit/s, 235.28 Mbit/s, and 152.27 Mbit/s, respectively at the edge of the system for six users. The proposed NOMA attained an achievable sum rate of 18.36% and 65.98% as compared with the NGDPA approaches and GRPA approaches in the 4×4 MIMO-based Visible Light Communication networks with eight uniformly distributed users. Generally, as the number of users increases in the considered system coverage, the total sum rate declines. But, the proposed NOMA has superior performance than GRPA and NGDPA. In conclusion, the results implied that MIMO-NOMA was promising for multi-user visible light communication system.

6.2   Recommendations

Having many users in the MIMO-NOMA-based visible light communication system and assigning all users to a similar resource block can be problematic. The user with the best channel condition must decode signals of all users before decoding his/her own signal. This makes delays in decoding and results in high complexity. As a result, future works can focus on finding

optimal user grouping and allocating the power to each group.

Additionally, not all users require the same amount of data rates. Some users need a high data rate, and others may not. Some users may use data for video, and others may use it for exploring websites. Therefore, allocating the power according to quality of service needs is an open research problem in MIMO-NOMA-based visible light communication networks.

References

[1] H. Haas, "LiFi: Conceptions, Misconceptions, and Opportunities," *IEEE Photonics Conf.*, pp. 680–681, 2016.

[2] Cisco, "Cisco Annual Internet Report(2018–2023)," Technical report, Cisco, 2020.

[3] S. Shao and A. Khreishah, "Delay Analysis of Unsaturated Heterogeneous Omnidirectional-Directional Small Cell Wireless Networks," *IEEE Trans. Wirel. Commun.*, vol. 99, p. 1, 2016.

[4] K. Saha, V. V. Vira, A. Garg, D. Koutsonikolas, "A feasibility study of 60 GHz indoor WLANs," *In Computer Communication and Networks (ICCCN), 2016 25th International Conference, IEEE*, pp. 1-9, 2016.

[5] N. Al-Falahy and O. Y. Alani, "Potential technologies to 5G network: challenges and opportunities," *IT Professional*, vol. 19, no. 1, pp. 12-20, 2017.

[6] A. Tzanakaki et al., "Wireless-Optical Network Convergence: Enabling the 5G Architecture to Support Operational and End-User Services," *IEEE Communications Magazine*, vol. 55, no. 10, pp. 184-192, Oct. 2017.

[7] H. Zhang, S. Chen, H. J. X. Li, and X. Du, "Interference Management for Heterogeneous Networks with Spectral Efficiency Improvement," *IEEE Wirel. Commun.*, vol. 22, pp. 101–107, 2015.

[8] A. Khreishah, S. Shao, A. Gharaibeh, M. Ayyash, H. Elgala and N. Ansari, "A Hybrid RF-VLC System for Energy Efficient Wireless Access," *IEEE Transactions on Green Communications and Networking*, vol. 2, no. 4, pp. 932-944, Dec. 2018.

[9] H. Haas, C. Chen, and Y. Wang, "What is lifi?," *Light. Technol.*, vol. 34, no. April, pp. 1533–1544, 2016.

[10] A. Benjebbour, Y. Saito, Y. Kishiyama, A. Li, A. Harada and T. Nakamura, "Concept and practical considerations of non-orthogonal multiple access (NOMA) for future radio

access," *2013 International Symposium on Intelligent Signal Processing and Communication Systems*, 2013, pp. 770-774.

[11] Ding, M. Peng and H. V. Poor, "Cooperative Non-Orthogonal Multiple Access in 5G Systems," *IEEE Communications Letters*, vol. 19, no. 8, pp. 1462-1465, Aug. 2015.

[12] S. Arnon, J. Barry, and G. Karagiannidis, Advanced Optical Wireless Communication Systems.Cambridge, U.K.: Cambridge Univ. Press, 2012.

[13] L. Zeng et al., "High data rate multiple-input multiple-output (MIMO) optical wireless communications using white led lighting," *IEEE Journal on Selected Areas in Communications*, vol. 27, no. 9, pp. 1654-1662, December 2009.

[14] J.-Y. Sung, C.-H. Yeh, C.-W. Chow, W.-F. Lin, and Y. Liu, "Orthogonal frequency-division multiplexing access (OFDMA) based wireless visible light communication (VLC) system," *Opt. Commun.*, vol. 355, pp. 261-268, Nov. 2015.

[15] L. Dai, B. Wang, Y. Yuan, S. Han, C.-L. I, and Z. Wang, "Non-orthogonal multiple access for 5G: Solutions, challenges, opportunities, and future research trends," *IEEE Commun. Mag.*, vol. 53, no. 9, pp. 74-81, Sep. 2015.

[16] Z. Ding, Z. Yang, P. Fan, and H. V. Poor, "On the Performance of Non-Orthogonal Multiple Access in 5G Systems with Randomly Deployed Users," *IEEE Signal Processing Letters*, vol. 21, no. 12, pp. 1501-1505, Dec. 2014.

[17] H. Marshoud, V. M. Kapinas, G. K. Karagiannidis, and S. Muhaidat, "Non-orthogonal multiple access for visible light communications," *IEEE Photon. Technol. Lett.*, vol. 28, no. 1, pp. 51–54, Jan. 1, 2016.

[18] S. Juneja and S. Vashisth, "Indoor positioning system using visible light communication," *2017 International Conference on Computing and Communication Technologies for Smart Nation (IC3TSN)*, pp. 79-83, 2017.

[19] X. Guan, Y. Hong, Q. Yang, and C. C.-K. Chan, "Non-orthogonal multiple access with phase pre-distortion in visible light communication," *Opt. Exp.*, vol. 24, no. 22, pp. 25816-25823, Oct. 2016.

[20] C. Chen, W. Zhong and D. Wu, "On the coverage of multiple-input multiple-output visible light communications [Invited]," *IEEE/OSA Journal of Optical Communications and Networking*, vol. 9, no. 9, pp. D31-D41, Sept. 2017.

[21] B. Lin, Z. Ghassemlooy, X. Tang, Y. Li, and M. Zhang, "Experimental demonstration of optical MIMO NOMA-VLC with single carrier transmission," *Optical Communication*, vol. 402, pp. 52–55, Nov. 2017.

[22] C. Chen, W. Zhong, H. Yang, and P. Du, "On the Performance of MIMO-NOMA-Based Visible Light Communication Systems," *IEEE Photonics Technology Letters*, vol. 30, no. 4, pp. 307-310, 15 Feb.15, 2018.

[23] C. Wang et al., "On the performance of the MIMO zero-forcing receiver in the presence of channel estimation error," *IEEE Transaction Wireless Communication*, vol. 6, no. 3, pp. 805-810, Mar. 2007.

[24] L. Yin et al., "Performance evaluation of non-orthogonal multiple access in visible light communication," *IEEE Trans. Commun.*, vol. 64, no. 12, pp. 5162-5175, Dec. 2016.

[25] H. Elgala, R. Mesleh, and H. Haas, "Indoor optical wireless communication: potential and state-of-the-art," *IEEE Commun. Mag.*, vol. 49, pp. 56-62, 2011.

[26] Z. Ghassemlooy, S. Arnon, M. Uysal, Z. Xu, and J. Cheng, "Emerging optical wireless communications-advances and challenges," *IEEE J. Sel. Areas Commun.*, vol. 33, pp. 1738-1749, 2015.

[27] A. Boucouvalas, P. Chatzimisios, Z. Ghassemlooy, M. Uysal, and K. Yiannopoulos, "Standards for indoor optical wireless communications," *IEEE Communications Magazine*, vol. 53, pp. 24-31, 2015.

[28] D. Karunatilaka, F. Zafar, V. Kalavally, and R. Parthiban, "LED-based indoor visible light communications: state of the art," *IEEE Commun. Surv. Tutorials*, vol. 17, pp. 1649-1678, 2015.

[29] Y. Zhang, H. Yu, J. Zhang, Y. Zhu, and J.Wang, "Space codes for MIMO optical wireless communications: error performance criterion and code construction," *IEEE Trans. Wirel. Commun.*, vol. 16, pp. 3072-3085, 2017.

[30] Z. Ghassemlooy, P. Luo, and S. Zvanovec, "Optical camera communications," *Opt. Wirel. Commun.*, pp. 547-568, 2017.

[31] F. Yang and J. Gao, "Dimming control scheme with high power and spectrum efficiency for visible light communications," *IEEE Photonics J.*, vol. 9, pp. 1-12, 2017.

[32] M. Z. Chowdhury, T. Hossan, and Y. M. Jang, "A Comparative Survey of Optical Wireless Technologies: Architectures and Applications," *IEEE Access*, pp. 2169-3536, 2018.

[33] S. U. Rehman, S. Ullah, P. Han, J. Chong, and S. Yongchareon, "Visible Light Communication: A System Perspective -Overview and Challenges," *MDPI*, pp. 1-22, 2019.

[34] H. Marshoud et al., "On the performance of visible light communication systems with non-orthogonal multiple access," *IEEE Trans. Wireless Commun.* 16(10), 6350-6364 (2017).

[35] H. Marshoud, S. Muhaidat, P. C. Sofotasios, S. Hussain, M. A. Imran and B. S. Sharif, "Optical Non-Orthogonal Multiple Access for Visible Light Communication," *IEEE Wireless Communications*, vol. 25, no. 2, pp. 82-88, April 2018.

[36] S. Rajagopal, R. D. Roberts and S. Lim, "IEEE 802.15.7 visible light communication: modulation schemes and dimming support," *IEEE Communications Magazine*, vol. 50, no. 3, pp. 72-82, March 2012.

[37] X. Deng, S. Mardanikorani, G. Zhou and J. -P. M. G. Linnartz, "DC-Bias for Optical OFDM in Visible Light Communications," *IEEE Access*, vol. 7, pp. 98319-98330, 2019.

[38] S. H. Yu, O. Shih, H. M. Tsai, N. Wisitpongphan, and R. D. Roberts, "Smart automotive lighting for vehicle safety," *IEEE Commun.* Mag., vol. 51, no. 12, pp. 50-59, 2013.

[39] M. Uysal, F. Miramirkhani, O. Narmanlioglu, T. Baykas, and E. Panayirci, "IEEE 802.15.7r1 reference channel models for visible light communications," *IEEE Commun. Mag.*, vol. 55, no. 1, pp. 212-217, 2017.

[40] Z. Wang, Q. Wang, W. Huang, and Z. Xu, "Visible Light Communications: Modulation and Signal Processing," *IEEE Photonics J.*, pp. 10-12, 2017.

[41] Z. Ding, M. Xu, Y. Chen, M. Peng, and H. Poor Vincent, "Embracing Non-Orthogonal Multiple Access in Future Wireless Networks," *Technol Electron Eng.*, pp. 322-339, 2018.

[42] W. Liang, Z. Ding, and H. V. Poor, "Non-Orthogonal Multiple Access (NOMA) for 5G Systems," Columbia University Press, 2017.

[43] J. Choi, "Power allocation for max-sum rate and max-min rate proportional fairness in NOMA," *IEEE Commun. Lett.*, vol. 20, no. 10, pp. 2055-2058, 2016.

[44] Y. Saito, A. Benjebbour, and Y. Kishiyama, "System-level performance evaluation of downlink non-orthogonal multiple access (NOMA)," *IEEE 24th Int Symp Pers. Indoor Mob. Radio Commun.*, pp. 611-615, 2013.

[45] N. Nonaka, A. Benjebbour, and K. Higuchi, "System-level throughput of NOMA using intra-beam superposition coding and SIC in MIMO downlink when channel estimation error exists," *IEEE International Conference on Communication System*, pp. 202-206, 2014.

[46] X. Deng, S. Mardanikorani, G. Zhou and J. -P. M. G. Linnartz, "DC-Bias for Optical OFDM in Visible Light Communications," *IEEE Access*, vol. 7, pp. 98319-98330, 2019.

[47] J. M. Kahn, R. You, P. Djahani, A. G. Weisbin, Beh Kian Teik, and A. Tang, "Imaging diversity receivers for high-speed infrared wireless communication," *IEEE Communications Magazine*, vol. 36, no. 12, pp. 88-94, 1998.

[48] P. H. Pathak, X. Feng, P. Hu and P. Mohapatra, "Visible Light Communication, Networking, and Sensing: A Survey, Potential and Challenges," *IEEE Communications Surveys & Tutorials*, vol. 17, no. 4, pp. 2047-2077, Fourthquarter 2015.

[49] X. Li, J. Vucic, V. Jungnickel, and J. Armstrong, "On the Capacity of Intensity-Modulated Direct-Detection Systems and the Information Rate of ACO-OFDM for In-

door Optical Wireless Applications," *IEEE Transactions on Communications*, vol. 60, no. 3, pp. 799-809, March 2012.

[50] H. Parikh, J. Chokshi, N. Gala and T. Biradar, "Wirelessly transmitting a grayscale image using visible light," *2013 International Conference on Advances in Technology and Engineering (ICATE)*, pp. 1-6,2013.

[51] A. Burton, H. Le Minh, Z. Ghassemlooy, E. Bentley and C. Botella, "Experimental Demonstration of 50-Mb/s Visible Light Communications Using 4×4 MIMO," *IEEE Photonics Technology Letters*, vol. 26, no. 9, pp. 945-948, May1, 2014.

[52] K. Cui, G. Chen, Z. Xu and R. D. Roberts, "Line-of-sight visible light communication system design and demonstration," *2010 7th International Symposium on Communication Systems, Networks & Digital Signal Processing (CSNDSP 2010)*, pp. 621-625, 2010.